Journal of Neuroinflammation

RESEARCH

Open Access

Glyphosate exposure exacerbates neuroinflammation and Alzheimer's disease-like pathology despite a 6-month recovery period in mice

Samantha K. Bartholomew[1,2], Wendy Winslow[1], Ritin Sharma[3,4], Khyatiben V. Pathak[3,4], Savannah Tallino[1,2], Jessica M. Judd[1], Hector Leon[1], Julie Turk[1], Patrick Pirrotte[3,4*†] and Ramon Velazquez[1,2*†]

Abstract

Background Glyphosate use in the United States (US) has increased each year since the introduction of glyphosate-tolerant crops in 1996, yet little is known about its effects on the brain. We recently found that C57BL/6J mice dosed with glyphosate for 14 days showed glyphosate and its major metabolite aminomethylphosphonic acid present in brain tissue, with corresponding increases in pro-inflammatory cytokine tumor necrosis factor-α (TNF-α) in the brain and peripheral blood plasma. Since TNF-α is elevated in neurodegenerative disorders such as Alzheimer's Disease (AD), in this study, we asked whether glyphosate exposure serves as an accelerant of AD pathogenesis. Additionally, whether glyphosate and aminomethylphosphonic acid remain in the brain after a recovery period has yet to be examined.

Methods We hypothesized that glyphosate exposure would induce neuroinflammation in control mice, while exacerbating neuroinflammation in AD mice, causing elevated Amyloid-β and tau pathology and worsening spatial cognition after recovery. We dosed 4.5-month-old 3xTg-AD and non-transgenic (NonTg) control mice with either 0, 50 or 500 mg/kg of glyphosate daily for 13 weeks followed by a 6-month recovery period.

Results We found that aminomethylphosphonic acid was detectable in the brains of 3xTg-AD and NonTg glyphosate-dosed mice despite the 6-month recovery. Glyphosate-dosed 3xTg-AD mice showed reduced survival, increased thigmotaxia in the Morris water maze, significant increases in the beta secretase enzyme (BACE-1) of amyloidogenic processing, amyloid-β (Aβ) 42 insoluble fractions, Aβ 42 plaque load and plaque size, and phosphorylated tau (pTau) at epitopes Threonine 181, Serine 396, and AT8 (Serine 202, Threonine 205). Notably, we found increased pro- and anti-inflammatory cytokines and chemokines persisting in both 3xTg-AD and NonTg brain tissue and in 3xTg-AD peripheral blood plasma.

†Patrick Pirrotte and Ramon Velazquez are co-senior authors.

*Correspondence:
Patrick Pirrotte
ppirrotte@tgen.org
Ramon Velazquez
Rvelazq3@asu.edu

Full list of author information is available at the end of the article

Conclusion Taken together, our results are the first to demonstrate that despite an extended recovery period, exposure to glyphosate elicits long-lasting pathological consequences. As glyphosate use continues to rise, more research is needed to elucidate the impact of this herbicide and its metabolites on the human brain, and their potential to contribute to dysfunctions observed in neurodegenerative diseases.

Keywords Glyphosate, Aminomethylphosphonic acid, Alzheimer's disease, Neuroinflammation, 3xTg-AD mice

Introduction

The increased prevalence of neurodegenerative disorders such as Alzheimer's Disease (AD) is alarming given that more than 6.7 million people are affected with this disorder in the US alone, and this number may reach 14 million Americans by 2060 [1]. People with AD present with severe memory loss, diminished decision-making abilities, and other behavioral changes that affect their everyday life [1]. The key pathologies present in AD that subsequently disrupt neuronal function leading to cognitive deficits include the accumulation of (1) extracellular amyloid beta (Aβ) plaques, (2) intracellular neurofibrillary tau tangles (NFT), and (3) neuroinflammation [1–3]. An abundance of work highlights that environmental factors play a role in sporadic AD, which accounts for >95% of those affected with AD overall [4, 5]. Factors such as air pollution, diet, exposure to toxins, and infection are known to result in elevated levels of inflammation [6] and oxidative stress, both of which can increase a person's risk of developing AD and other neurodegenerative disorders [4–6].

Herbicides are a ubiquitous part of our environment that may consequently pose harm to human health. Glyphosate (*N*-(phosphonomethyl) glycine) is the most heavily-applied herbicide in the US [7]. Approximately 300 million pounds are used annually in agricultural communities throughout the US [8]. Glyphosate works by inhibiting the enzyme enolpyruvylshikimate-3-phosphate in the shikimate pathway of plants preventing the production of aromatic amino acids critical for survival [9]. As of 2020, the US Environmental Protection Agency (EPA) stated that glyphosate poses no risks of concern to human health. However, the World Health Organization's International Agency for Research on Cancer classified the herbicide as "possibly carcinogenic to humans" [10]. More recent research has highlighted that cancer may not be the only disease linked to glyphosate exposure [11], with multiple reports deciphering the effects of glyphosate on various organs and tissues, including the brain [6, 12, 13]. A recent publication from our group demonstrated that glyphosate could cross the blood brain barrier (BBB), being detected in brain tissue of exposed mice, and can elevate pro-inflammatory cytokines such as tumor necrosis factor-α (TNF-α) [6]. Additionally, follow-up work from others has identified that glyphosate can, via elevated pro-inflammatory cytokines, disrupt mechanisms important for synaptic strengthening such as long-term potentiation [13]. Notably, a recent report found that 83.87% of humans included in the NHANES study had detectable urinary levels of glyphosate, with higher levels associated with decreased cognition [14]. Collectively, these findings suggest that there is an urgent need to understand the role of this herbicide in brain-related dysfunction.

Recent work demonstrates that glyphosate exposure may contribute to neuronal dysfunction, particularly via mechanisms linked to AD. In a recent study, a positive association was observed between urinary glyphosate and blood serum neurofilament light chain (NfL) levels [15]– NfL is a marker of neuronal axon damage, indicating that higher levels of glyphosate may be linked to neuronal damage [16]. Notably, the association was more pronounced in participants>40 years of age and with a body mass index between 25 and 30 – subgroups with an increased risk for AD [1]. NfL is a blood biomarker that predicts cognitive decline across the AD continuum [16]. Additionally, previously published work demonstrated that glyphosate exposure to primary cortical neurons from the APP/PS1 mouse model of AD resulted in increased soluble Aβ levels [6]. These findings collectively highlight that more work is needed to determine the impact of glyphosate exposure on mechanisms associated with AD.

Due to the lack of a shikimate pathway in mammals, it has been suggested that ingested glyphosate is eliminated virtually unmetabolized [17–19]. However, recent studies have found that the gut microbiota can metabolize glyphosate into its major metabolite, aminomethylphosphonic acid [20, 21]. Additionally, chronic neuroinflammation can significantly alter cellular mechanisms important for behaviors such as learning and memory [22] and may contribute to neurodegenerative diseases where neuroinflammation is rampant [23, 24]. Given this, an important question that remains to be investigated is whether glyphosate and aminomethylphosphonic acid remain in the brain at detectable levels months after exposure has ceased. Evidence from prenatal exposure studies highlights that glyphosate exposure results in offspring with developmental delays, craniofacial abnormalities and cognitive deficits later in life, illustrating that early exposure can produce long-lasting consequences [25–27]. It remains to be known whether (1) glyphosate and aminomethylphosphonic acid remain in the brain after a recovery period and/or (2) an

exposure period during early adulthood produces long-term detrimental consequences. Given that glyphosate and aminomethylphosphonic acid can cross the BBB [6, 28], it needs to be determined whether these molecules can remain in the brain and accelerate pathologies such as neuroinflammation, Aβ, and tau pathology.

The goal of the current study was to determine the impact of glyphosate exposure for 13 weeks, starting in early adulthood, followed by a six-month recovery period. Specifically, we sought to determine whether glyphosate and aminomethylphosphonic acid remained in the brain, and hypothesized that despite recovery from glyphosate exposure, neuroinflammation and exacerbation of AD-like neuropathologies – and associated cognitive deficits – would be observed in the 3xTg-AD mouse model of AD.

Methods

Animals and study design

3xTg-AD homozygous mice were generated as previously described [29, 30]. C57BL6/129S6 mice were used as non-transgenic controls (NonTg). Notably, only female 3xTg-AD mice were used because males do not display consistent neuropathology [30, 31], and the use of males is cautioned against [32], consistent with published work using this model [30, 33–35]. Mice were kept on a 12-h light/dark cycle at 23 °C with ad libitum access to food and water and group-housed, 4–5 per cage. Mice were randomly assigned to one of three doses of glyphosate starting at 4.5 months of age. The start age of glyphosate exposure was selected to begin prior to the presence of Aβ plaques and tau pathogenesis, pathologies which are detectable in 3xTg-AD mice at 6 months of age [30, 33]. Dosing ceased at ~7.5 months of age, for a total of 13 weeks, which is classified as chronic exposure consistent with previous publications [12, 36]. All animals were aged to 12 months for behavioral testing (4.5 months after exposure), as Aβ and tau pathogenesis is extensive in cortical and hippocampal brain regions at this age in 3xTg-AD mice [30, 33], allowing us to assess if early glyphosate exposure exacerbated cognitive deficits, Aβ, and tau pathogenesis. Blood was collected from mice at 13.5 months of age, and all animals were subsequently euthanized for tissue harvesting, when pathology is well advanced in the 3xTg-AD mouse [33]. All animal procedures were approved in advance by the Institutional Animal Care and Use Committee of Arizona State University, protocol number 22-1933R.

Justification of glyphosate doses

As previously described by our group [6], chemically pure glyphosate (*N*-(Phosphonomethyl)glycine; $C_3H_8NO_5P$) was purchased from Sigma-Aldrich (product number P9556) and prepared at 0.107 g/L in 1.89 M sodium hydroxide. The stock solution was serially diluted with deionized (DI) water to the desired doses and adjusted to a pH of 7, with the same solution without glyphosate serving as a vehicle. Mice were randomly assigned to receive one of three doses starting at 4.5 months of age: vehicle (0 mg/kg), 50 mg/kg, or 500 mg/kg of body weight. Mice were dosed daily over the course of the 13-week exposure period. The high dose (500 mg/kg) was based on the no observable adverse effect limit (NOAEL) for chronic (90 day) exposure in mice established by the EPA [37], and has been used in publications to determine the effects of glyphosate exposure on neurocognitive and peripheral organ alterations [12, 36, 38, 39]. The lower dose of 50 mg/kg was selected as it is 10 fold less than the NOAEL [37], and is less than the value that was used to calculate the chronic reference dose for humans of 1.75 mg/kg/day [37], which was 175 mg/kg [40]. This allows us to compare our results to previous published work assessing glyphosate exposure and neurocognitive effects [12, 36, 38]. The number of mice per group was 0 mg/kg ($n=14$ 3xTg-AD; $n=15$ NonTg), 50 mg/kg ($n=13$ 3xTg-AD; $n=15$ NonTg), and 500 mg/kg ($n=15$/group for both 3xTg-AD and NonTg). The number of mice used for each analysis was similar to previous published work [31, 33, 41].

Behavior testing

At 12 months of age, all mice were tested in the Morris water maze (MWM) task to assess hippocampal-dependent spatial learning and memory, as previously described [42, 43]. All animals underwent 4 training trials/day for 5 days. The location of the hidden platform remained constant, but the start location pseudo-randomly varied across trials. Mice were given 60 s/trial to locate the hidden platform. Twenty-four hours after the last training session, the platform was removed, and mice were returned to the MWM for 60 s to assess spatial reference memory. Data were collected with EthoVisionXT (Noldus Information Technology).

Blood collection and plasma extraction

Blood was collected via the submandibular vein prior to euthanasia at 13.5 months of age. 150–200 µL (≤1% of the subject's body weight) of blood was collected and placed into EDTA-lined tubes (BD K_2EDTA #365974) and inverted eight times to assure anticoagulation. Tubes were kept on ice for 60–90 min and then centrifuged at 455 g for 30 min at 4 °C to separate phases. The top layer was collected and frozen at −80 °C.

Circulatory glyphosate and aminomethylphosphonic acid quantification

Glyphosate and aminomethylphosphonic acid were in a concentration range of 0–3 ng/mL in plasma, and

quantified as follows: briefly, pooled lyophilized human plasma (Innovative research, Novi, MI) was used for preparing calibration curves and quality controls by spiking variable concentrations of glyphosate and aminomethylphosphonic acid. Calibration curves, quality controls and mouse plasma (5–20 µL) spiked with internal standards ($^{13}C^{15}N$ glyphosate and $^{13}C^{15}N$ aminomethylphosphonic acid at 6.26 ng/mL concentration) were subjected to protein removal using 500 µL 10 kDa molecular weight cut off (MWCO, Millipore Sigma, Burlington, MA) spin columns (10,000 g, 20 min, 4 ℃). The filtrate was acidified with formic acid to a final concentration of 0.1% (v/v) and used for Liquid chromatography tandem mass spectrometry (LC-MS/MS) analysis. Plasma measurements showed excellent linearity with an $R^2 > 0.99$ (Supplemental Fig. 1), and precision < 15% relative standard deviation (RSD), and accuracy > 87% for both glyphosate and aminomethylphosphonic acid. The observed lower limit of quantitation (LOD) and limit of quantitation (LOQ) were 10 pg/mL and 50 pg/mL for glyphosate and aminomethylphosphonic acid, respectively.

Tissue harvesting and processing, western blots, and enzyme-linked immunosorbent assay (ELISA)

Mice were euthanized at an average age of 13.5 months. All mice were perfused with fresh 1X Phosphate buffered saline (PBS) to remove blood from the brain. Brains were extracted and the left hemisphere was fixed in 4% paraformaldehyde for 48 h; from the right hemisphere, we isolated the entire cerebral cortex, then removed the hippocampus (Hp). The cortex (Ctx) fraction represents the cortical plate – including the isocortex, olfactory areas, and retrohippocampal cortex – and the cortical subplate. Dissected Ctx tissue was prioritized for glyphosate, aminomethylphosphonic acid and cytokine/chemokine measures, where Hp tissue was not, due to the limited amount of sample compared to the Ctx. The Hp and remaining Ctx were prioritized for Aβ and pathological tau measures, given that a major goal was to determine AD-like pathology exacerbation effects with early glyphosate exposure in key areas affected in AD. Hp and Ctx tissue were prepared for protein assays as previously described [42, 43]. Dissected tissue was homogenized in tissue protein extraction reagent supplemented with protease (Roche Applied Science, IN, USA) and phosphatase inhibitors (Millipore, MA, USA). The homogenized tissues were centrifuged at 21,130 g at 4 °C for 30 min, and the supernatant (soluble fraction) was stored at −80 °C. We then homogenized the pellet in 70% formic acid followed by centrifuging at 4 ℃ for 30 min, to extract insoluble proteins. Western blots were performed under reducing conditions as previously described [44], using the following antibodies: Biolegend, 6E10 (Full length (FL)-amyloid precursor protein (APP), Catalog #9320-02, 1:1,000); Abcam, Glyceraldehyde 3-phosphate dehydrogenase (GAPDH, Catalog #ab8245, 1:3,000). Licor Image Studio software was used for quantitative analyses by normalizing the intensity of the protein of interest with its loading control GAPDH within each blot. Mean density values were normalized for each immunoblot by dividing each experimental band density by the mean 3xTg-AD 0 mg/kg density for the Hp and Ctx. The experimenter was blinded to the group allocations. Soluble fractions of Hp protein homogenates were probed for 99 amino acid C-terminal fragment of amyloid precursor protein (C99, MyBioSource catalog #MBS7612253) and Beta-secretase 1 (BACE-1, LSBio catalog# LS-F7271) using commercially available ELISA kits. Soluble and insoluble fractions of Hp and Ctx were probed for human $Aβ_{40}$ and $Aβ_{42,}$ and phosphorylated tau (pTau) at Threonine 181 (Thr 181) and Serine 396 (Ser 396) residues, using the commercially available ELISA kits (Invitrogen-ThermoFisher Scientific catalog #KMB3481, KMB3441 and KHB7031, respectively) as previously described [42]. All samples were run in duplicate wells.

Brain glyphosate and aminomethylphosphonic acid measurements

Glyphosate and aminomethylphosphonic acid measurements were conducted as previously described [6]. Samples were spiked-in with 10 ng/g of $^{13}C_2{}^{15}N$ glyphosate (Toronto Research Chemicals) and $^{13}C^{15}N$ aminomethylphosphonic acid (Toronto Research Chemicals). Lipid removal was carried using 1 cc Sep-Pak C18 solid phase cartridges (Waters, Milford-MA) and the flow-through (400 µL) were acidified with formic acid. Samples, calibration curve standards and quality control standards in 50 or 100 µL injection volume were analyzed by liquid chromatography with multiple reaction monitoring (LC-MRM) on Vanquish Duo Ultra high-pressure liquid chromatography (UHPLC) system coupled to a Thermo TSQ Altis instrument [6, 45]. Calibration curves performed in the mouse brain matrix over a range of 0–60 ng/g of glyphosate and aminomethylphosphonic acid showed excellent linearity ($R^2 > 0.99$, Supplementary Fig. 2). The observed LOQ for the assay defined as the lowest spiked-in standard with a mean accuracy between 80 and 120% and precision less than 20% RSD was 0.4 ng/g for glyphosate and aminomethylphosphonic acid respectively [6, 46].

Multiplex cytokine assay

The long-lasting inflammatory effects of glyphosate were tested in blood plasma and cortical protein homogenates using a Bio-Plex mouse cytokine 23-plex kit (Bio-Rad, Catalog #M60009RDPD). Briefly, 15 µl of plasma were diluted in 35 µl diluent solution per assay instructions. Soluble cortical protein homogenates containing

100 µg total protein per well were added in duplicate to a 96-well plate and assayed according to manufacturer's instructions. Measurements were calculated with the Bio-Plex Manager software. Standard curves were plotted using five-parameter logistic regression and concentrations were calculated accordingly. Levels that were not detected based on manufacture limits were not included in the statistical analysis.

Tissue sectioning, histology and ImageJ analysis

Brain hemispheres were sectioned into 50 µm coronal sections using a vibratome and stored in 1X PBS with 0.02% sodium azide. For $A\beta_{42}$ staining, one section per animal including the ventral extent of the Hp underwent immunohistochemistry as previously described [44], using an antibody to stain for $A\beta_{42}$ plaques (anti-$A\beta_{42}$, 1:200 dilution, Millipore, catalog# 5078P). Sections were permeabilized in 88% formic acid for 7 min before incubation in primary antibody. Brightfield photomicrographs were taken at 5x with a Zeiss Axio Imager, stitched together in Adobe photoshop and analyzed via ImageJ analyze particle function at a threshold of 0/70 as previously described [47]. For Thioflavin S staining, four sections per animal including the ventral extent of the Hp were included for analysis. Tissue sections were incubated in 4% paraformaldehyde for 15 min, filtered 1% aqueous Thioflavin S for 10 min at room temperature, washed twice in 80% ethanol, once in 95% ethanol, and 3 times in double distilled H2O. Images were taken at 5x on a fluorescence microscope (Leica DMi8) with Leica Application Suite X (LAS X) software, and quantified using ImageJ for % area of particles in the Hp as previously described [42, 48]. AT8 immunohistochemistry was performed as previously described [42, 43] with an antibody to stain cells expressing tau at Ser 202, Thr 205 (1:500 dilution, Invitrogen, catalog# MN1020). A series of coronal tissue sections including the dorsal and ventral extent of the Hp were evaluated for AT8, rendering seven sections per animal.

Unbiased stereology for AT8 + neuron quantification

Stereoinvestigator software V17 (Micro-BrightField, Cochester, VT) optical fractionator method was used to quantify AT8 + cornu ammonis 1 (CA1) cells in the Hp as previously described [42, 43]. Counts were performed at predetermined intervals; grid size (X and Y = 158 µm), counting frame (X and Y = 50 µm), superimposed on the live image of the tissue sections. Coronal tissue sections were analyzed using a $63x \times 1.4$ PlanApo oil immersion objective. Gunderson's scores remained ≤ 0.07. The average tissue thickness was 18.6 µm. Dissector height was set at 15 µm, with a 2-µm top and 2-µm bottom guard zone. Bright-field photomicrographs were taken with a Zeiss Axio Imager. The AT8 antibody penetrated the full depth of the section, allowing for an equal probability of counting all objects.

Statistical analysis

Two-way factorial Analysis of variance (ANOVA; for genotype and dose) was used to analyze experimental data, followed by recommended corrected post hoc tests when appropriate using Graph Pad PRISM (Version 10). Repeated measures ANOVA was used to analyze the MWM data output. One-way ANOVA was utilized for comparison of 3xTg-AD mice at the three doses for neuropathological measures solely present in humanized mice. Violation of homogeneity of variance was followed by non-parametric analysis. Statistical outliers were identified using the ROUT and Grubbs method. Significance was set at $p < 0.05$.

Results

Glyphosate exposure for 13 weeks followed by a 6-month recovery does not alter body weight but increases incidence of premature death

To determine whether exposure to glyphosate followed by recovery results in exacerbated neuroinflammation, neuropathology, and associated cognitive deficits, we exposed NonTg and 3xTg-AD mice to either 0 mg/kg (n = 14 3xTg-AD; n = 15 NonTg), 50 mg/kg (n = 13 3xTg-AD; n = 15 NonTg), or 500 mg/kg/day (n = 15/group) of glyphosate via oral gavage for 13 weeks starting at 4.5 months of age. At ~ 7.5 months of age, for the recovery period, dosing ceased for the remainder of life (Fig. 1A). The body weight of mice during the dosing period did not change (Fig. 1B, C). During the recovery period, between 7.5 and 13.5 months of age, and consistent with published work [30, 42], we found a significant main effect of genotype in % weight change, where the 3xTg-AD mice gained significantly more weight than the NonTg counterparts ($F_{(1,70)} = 7.914$, $p = 0.0064$; Fig. 1D). Lastly, we examined premature deaths during the dosing period and found that n = 1 NonTg 0 mg/kg and n = 1 NonTg 500 mg/kg mice died (Fig. 1E). The remaining NonTg mice survived the remainder of the study. During the dosing period, n = 1 3xTg-AD 0 mg/kg and n = 2 3xTg-AD 500 mg/kg mice died, and during the recovery period, n = 4 3xTg-AD 50 mg/kg and n = 2 3xTg-AD 500 mg/kg mice died (Fig. 1F, G). Collectively, these results highlight that exposure to glyphosate does not affect body weight but contributed to premature death, in particular in the 3xTg-AD mice.

Glyphosate exposure increases thigmotaxia in the Morris water maze task in 3xTg-AD mice

To determine whether glyphosate exposure impaired spatial cognition, mice were tested in the MWM for 6 consecutive days (0 mg/kg n = 13 3xTg-AD, n = 14 NonTg;

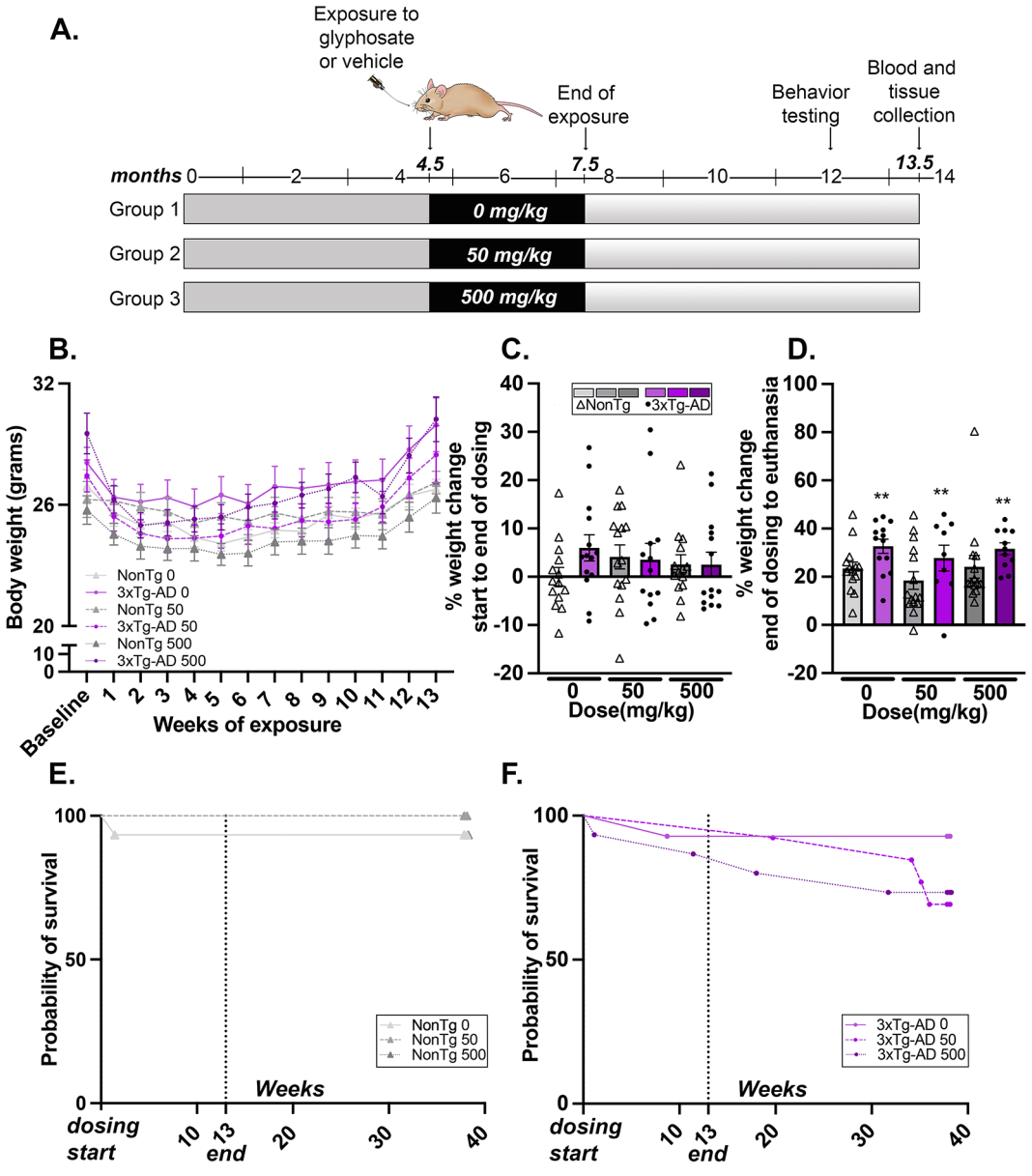

G.

Study groups	# of mice starting the study	# of mice that died during the dosing phase	# of mice that died during the recovery phase	Total # of mice completing the study
1. NonTg 0mg/kg	15	1	0	14
2. NonTg 50mg/kg	15	0	0	15
3. NonTg 500mg/kg	15	1	0	14
4. 3xTg-AD 0mg/kg	14	1	0	13
5. 3xTg-AD 50mg/kg	13	0	4	9
6. 3xTg-AD 500mg/kg	15	2	2	11

Fig. 1 Glyphosate exposure followed by a recovery period does not impact body weight but reduces survival in 3xTg-AD mice. (**A**) Experimental design. (**B**) Body weight across the dosing period. (**C**, **D**) % weight change during the dosing period, and % weight change during the recovery phase (end of dosing to end of study). (**E**, **F**) Survival curves during the dosing and recovery period. (**G**) Summary table of the number of mice at the start and conclusion of the study. Line and bar graphs are means ± SEM. $^{**}p < 0.01$

50 mg/kg $n=12$ 3xTg-AD, $n=15$ NonTg; 500 mg/kg $n=12$ 3xTg-AD, $n=14$ NonTg). During the first 5 training days, mice received 4 trials/day. We found a significant main effect of day in distance traveled to find the hidden platform, indicating learning ($F_{(4,\ 74)}=35.884$, $p<0.0001$; Fig. 2A). We also found a significant main effect of genotype ($F_{(1,\ 74)}=16.670$, $p=0.0001$), where 3xTg-AD mice traveled significantly further to find the hidden platform than NonTg mice. No significant dose main effects or interactions were found for distance. We next performed analysis of % thigmotaxia, the tendency to remain near walls. Notably, thigmotaxia has been identified as an indicator of anxiety [49]. During the learning phase, we found a significant effect of day ($F_{(1,\ 74)}=49.490$, $p<0.0001$; Fig. 2B), indicating that mice showed reduced % thigmotaxia across days. We also found a significant genotype by dose interaction ($F_{(2,\ 74)}=3.463$, $p=0.0365$). Post hoc analysis revealed that the 3xTg-AD 500 mg/kg group exhibited more thigmotaxia during the learning phase of the MWM compared to the 3xTg-AD 0 mg/kg group ($p=0.0123$), indicating increased anxiety. On Day 6, the platform was removed, and mice were tested in a 60 s probe trial to assess spatial memory. We found a significant main effect of genotype ($F_{(1,\ 74)}=4.043$, $p=0.048$; Fig. 2C), where the 3xTg-AD mice crossed the platform location significantly less than the NonTg counterparts. We also found a significant main effect of genotype ($F_{(1,\ 74)}=9.778$, $p=0.0025$; Fig. 2D) for swim speed, where the 3xTg-AD mice showed increased velocity compared with the NonTg mice, indicating that any deficits in performance were not a result of impaired swim speed. These data indicate that 3xTg-AD mice exposed to glyphosate showed increased thigmotaxia, evident of exacerbated anxiety-like behavior, although overall performance was equal across the dosed groups.

Aminomethylphosphonic acid is detected in brain tissue despite months of glyphosate recovery

To determine whether glyphosate and aminomethylphosphonic acid remain present in blood and brain

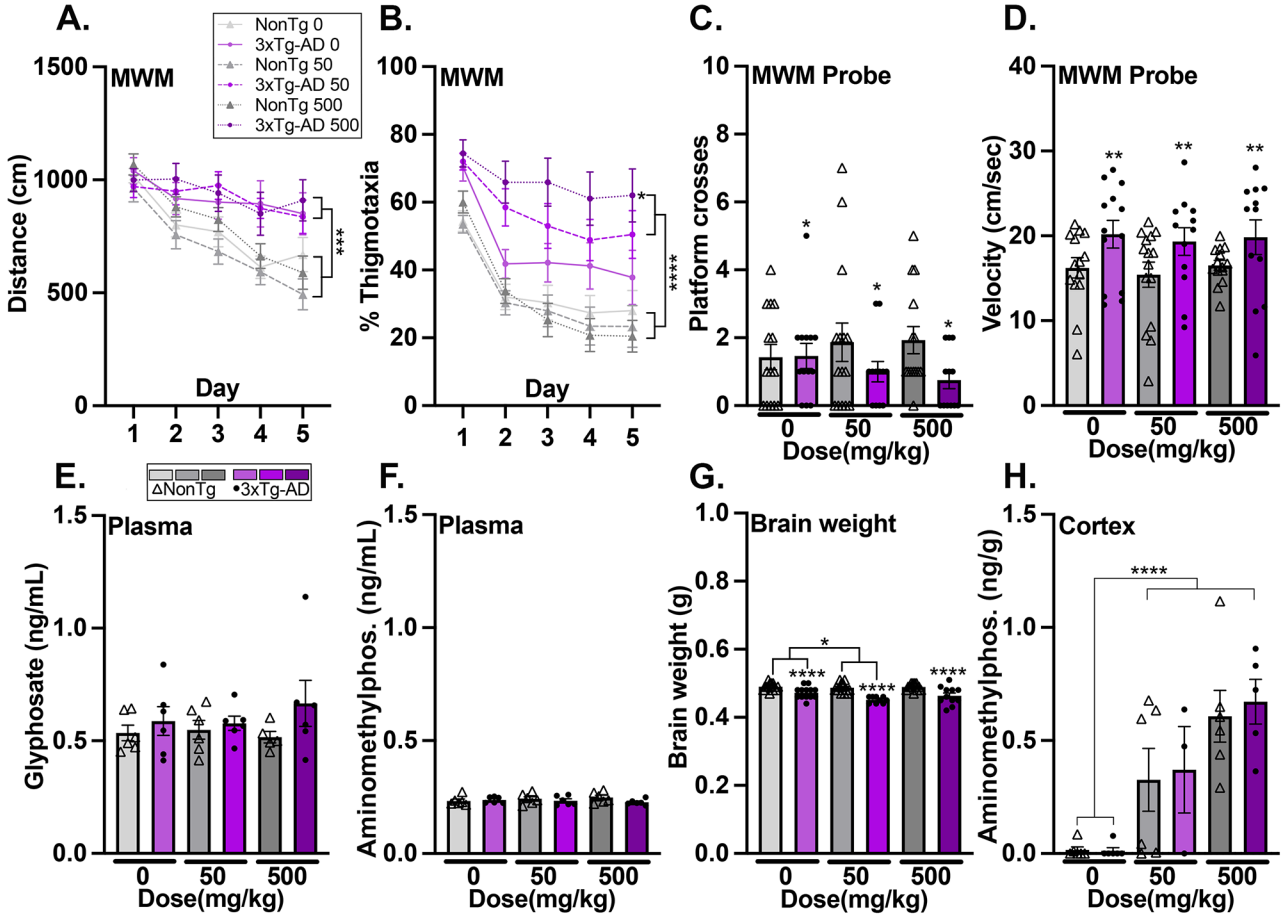

Fig. 2 Glyphosate exposure followed by a recovery period leads to the presence of aminomethylphosphonic acid in cortical tissue and increases thigmotaxia in the morris water maze (MWM). (**A**-**D**) Performance in the learning and memory phases of the MWM. (**E**, **F**) Glyphosate and aminomethylphosphonic acid in blood plasma of mice after the recovery period. (**G**) Brain weights of mice at the end of the study. (**H**) Aminomethylphosphonic acid was present months after glyphosate exposure in cortical brain tissue. Line and bar graphs are means ± SEM. *$p<0.05$, **$p<0.01$, ***$p<0.001$, ****$p<0.0001$

tissue months after exposure, we performed UPLC-MS on blood plasma and cortical tissue homogenates of mice (n=5–6/group). In blood plasma, while both glyphosate and aminomethylphosphonic acid were detected, likely resulting from glyphosate presence in chow, no significant differences between the groups were observed (Fig. 2E, F). When examining brain weight, we found a significant main effect of genotype, where the 3xTg-AD mice show significant reductions compared to the NonTg mice ($F_{(1,68)}$=51.83, p<0.0001; Fig. 2G), consistent with published work [30]. We also found a significant main effect of dose ($F_{(2, 68)}$=3.607, p=0.0325), where the 50 mg/kg dose had lower brain weight than the 0 mg/kg group (p=0.0277). We did not detect glyphosate in cortical tissue. Interestingly, we found a significant main effect of dose for cortical aminomethylphosphonic acid levels, where the 50- and 500 mg/kg groups had significantly higher levels than the 0 mg/kg regardless of genotype ($F_{(2,26)}$=20.81, p<0.0001; Fig. 2H). Collectively, these results highlight that 6 months after glyphosate exposure, brain weight is reduced in the 50 mg/kg groups and cortical aminomethylphosphonic acid is significantly elevated in mice at both 50 mg/kg and 500 mg/kg groups, highlighting lasting effects.

3xTg-AD glyphosate exposed mice show increased amyloidogenic processing and increased soluble and insoluble fractions of Aβ and plaques in the hippocampus (Hp) and cortex (Ctx)

Mice were euthanized at 13.5 months of age and brains were collected for neuropathological assessment. Given previous reports showing that glyphosate exposure increases amyloidosis in vitro [6], we first examined whether glyphosate exposure in vivo altered levels of full length human APP (n=4/group) and the C99 fragment of APP (n=6/group), which is cleaved to form the Aβ peptide. NonTg mice do not display humanized Aβ pathology and therefore were excluded from these analyses [42, 44]. We found no significant increase in steady state levels of APP in either Hp or Ctx tissue (Fig. 3A, B). For C99 in the Hp, we found a significant dose-dependent effect ($F_{(2,15)}$=62.26, p<0.0001; Fig. 3C), where 3xTg-AD 50 mg/kg (p<0.0001) and 500 mg/kg (p<0.001) mice showed higher levels than 0 mg/kg, and 500 mg/kg exhibited higher levels than the 50 mg/kg mice (p=0.0020). Next, we examined the levels of BACE-1 (n=6/group), the initiator enzyme that cleaves the transmembrane APP towards the amyloidogenic pathway [50]. We found a significant effect ($F_{(2, 15)}$=6.438, p=0.0096; Fig. 3D), where 3xTg-AD 50 mg/kg (p=0.0347) and 500 mg/kg (p=0.0061) mice showed a significant increase compared to the 3xTg-AD 0 mg/kg group, collectively highlighting an increase in the enzyme and cleaved product of the amyloidogenic pathway after the recovery period of glyphosate exposure.

To understand the effects of glyphosate exposure on AD pathogenesis, we used ELISAs to quantify soluble and insoluble $Aβ_{40}$ and $Aβ_{42}$ fractions in the 3xTg-AD mice (n=5–7/group). For soluble $Aβ_{40}$ fractions, we found no significant differences in the Hp and Ctx of 3xTg-AD mice across the doses (Fig. 3E). For insoluble $Aβ_{40}$ fractions, we found a significant effect ($F_{(2, 15)}$=5.305, p=0.0181; Fig. 3F), where the Hp of 3xTg-AD 500 mg/kg mice showed higher levels than the 3xTg-AD 0 mg/kg (p=0.0177) mice, but no significant differences were detected in the Ctx. Next, we examined the soluble fractions of $Aβ_{42}$ and found significant effects in the Hp ($F_{(2, 15)}$=9.726, p=0.0020; Fig. 3G), where the 500 mg/kg 3xTg-AD mice showed higher levels compared to the 0 mg/kg (p=0.0107) and 50 mg/kg (p=0.0028) groups. No differences in the Ctx were detected for soluble $Aβ_{42}$. For insoluble $Aβ_{42,}$ we found a significant dose-dependent effect in the Hp ($F_{(2,15)}$=75.06, p<0.0001; Fig. 3H), where the 3xTg-AD 500 mg/kg exhibited higher levels than the 3xTg-AD 50 mg/kg (p<0.0001), and 3xTg-AD 50 mg/kg showed higher levels than the 3xTg-AD 0 mg/kg mice (p=0.0418). Similarly, we found a significant dose-dependent effect of insoluble $Aβ_{42}$ in the Ctx ($F_{(2, 14)}$=46.58, p<0.0001), where the 3xTg-AD 500 mg/kg exhibited higher levels than the 3xTg-AD 50 mg/kg (p=0.0137), and 3xTg-AD 50 mg/kg showed higher levels than the 3xTg-AD 0 mg/kg mice (p<0.0001). $Aβ_{42}$ is more prone to aggregation and toxicity than $Aβ_{40}$ [51], thus we next quantified $Aβ_{42}$ plaque load and plaque (particle) size (n=5–6/group). We did not find any differences in the Hp for % change in $Aβ_{42}$ plaque load, however, we did find a significant effect of dose in the Ctx ($F_{(2,14)}$=4.675, p=0.0279; Fig. 3I, J), where the 3xTg-AD 500 mg/kg mice exhibited a higher load than the 50 mg/kg and 0 mg/kg counterparts (p=0.0440). We also found a significant effect in the Hp for plaque size ($F_{(2, 14)}$=6.126, p=0.0123; Fig. 3K), where the 3xTg-AD 50 mg/kg dosed mice had larger-sized plaques than the 0 mg/kg and 500 mg/kg counterparts. We found no significant effects in the Ctx for particle size. Lastly, we stained tissue for Thioflavin S to verify the extent of β-sheet confirmation aggregates in the ventral Hp of 3xTg-AD mice (n=5–6/group). We found a trending increase in the % area of particles in the Hp of 50 mg/kg and 500 mg/kg groups compared to 0 mg/kg groups $X^2_{(2)}$=5.440, p=0.0659 (Fig. 3L, M). Collectively, these results demonstrate that early glyphosate exposure alters APP processing, thereby exacerbating Aβ levels in key areas affected in AD, with most significant differences evident in insoluble $Aβ_{42}$ fractions, and $Aβ_{42}$ plaque load and plaque size, despite a 6-month recovery.

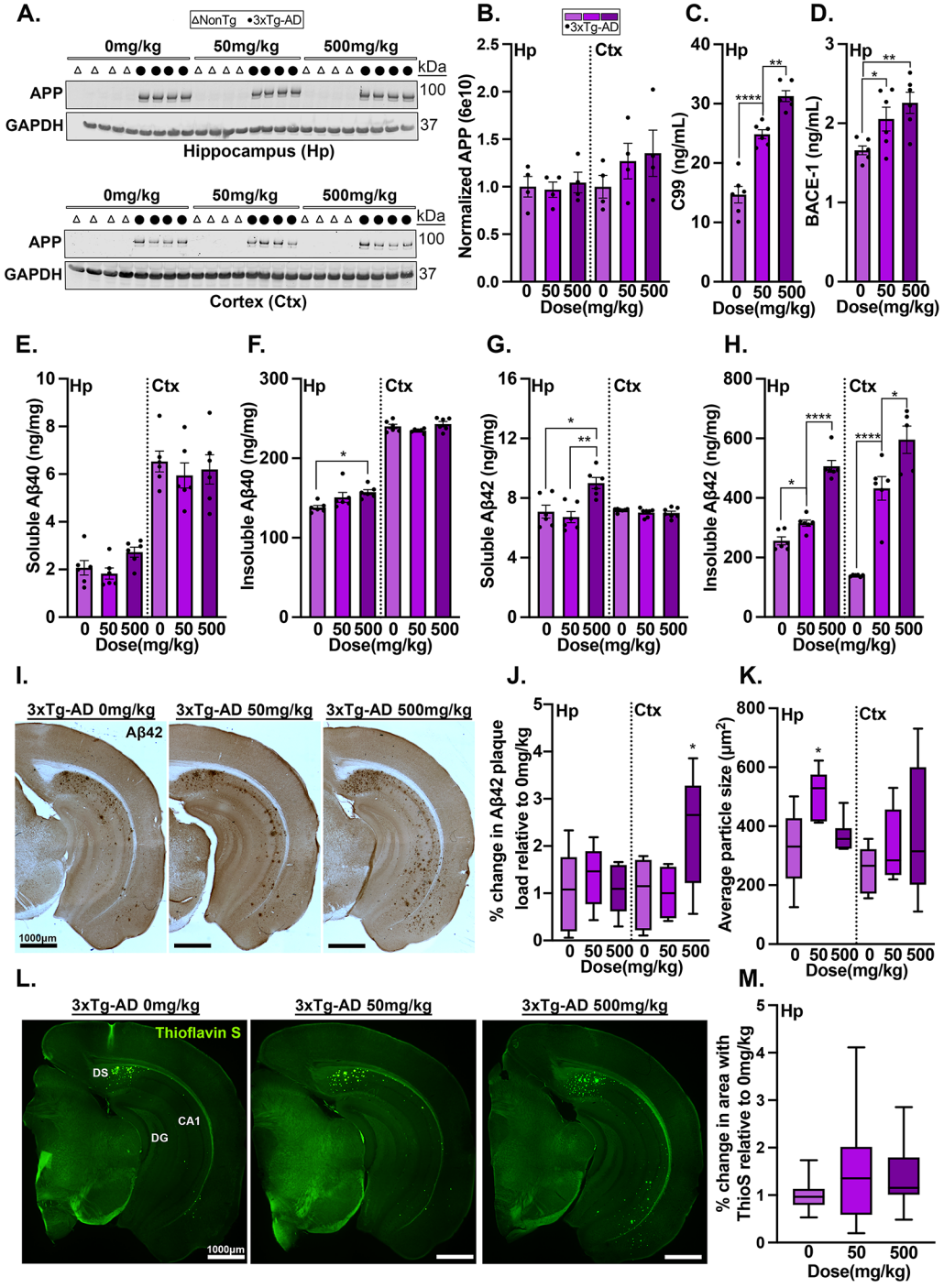

Fig. 3 Glyphosate exposure increases soluble and insoluble fractions of Aβ40 and 42, and Aβ42 plaque load by increasing cleavage products of the amyloid precursor protein despite a recovery period. (**A**, **B**) Representative western blot and quantification of full length APP (6e10) with loading control GAPDH in hippocampal (Hp) and cortex (Ctx) tissue. (**C**, **D**) Glyphosate exposure increases C99 and BACE-1 protein levels probed after the recovery period. (**E**-**H**) Soluble and insoluble fractions of Aβ40 and 42 in Hp and Ctx tissue. (**I**, **J**) Photomicrographs showing significant increases in both % Aβ42 plaque load in the Ctx of 3xTg-AD 500 mg/kg mice, and in average particle size in the Hp of 3xTg-AD 50 mg/kg mice. (**L**, **M**) Photomicrographs depicting Thioflavin S structures and quantification showing a trending increase in % particle area in glyphosate exposed 3xTg-AD mice ($p = 0.0659$) . *Abbreviations: DS = dorsal subiculum, DG = dentate gyrus, CA1 = cornus ammonis 1*. Bar graphs are means ± SEM. For box plots, the center line represents the median value, the limits represent the 25th and 75th percentile, and the whiskers represent the minimum and maximum value of the distribution.*$p < 0.05$, **$p < 0.01$, ****$p < 0.0001$

3xTg-AD glyphosate-exposed mice exhibit significantly increased pathological tau in the Hp and Ctx

We next sought to understand the long-lasting effects of glyphosate exposure on tau pathogenesis. To accomplish this, we performed ELISAs to detect soluble and insoluble fractions of phosphorylated tau (pTau) at Thr 181 and Ser 396 in 3xTg-AD mice (n=6/group). For soluble pTau Thr 181, we found a significant effect in the Hp ($F_{(2, 15)}$=25.54, p<0.0001; Fig. 4A), where both the 3xTg-AD 500 mg/kg (p<0.0001) and 50 mg/kg (p<0.0001) mice exhibited higher levels than the 3xTg-AD 0 mg/kg group. In the Ctx, we found a significant dose-dependent effect ($F_{(2, 15)}$=926.80, p<0.0001), where the 3xTg-AD 500 mg/kg exhibited higher levels than the 3xTg-AD 50 mg/kg (p<0.0001), and 3xTg-AD 50 mg/kg showed higher levels than the 3xTg-AD 0 mg/kg mice (p<0.0001). For soluble pTau Ser 396, we found significant dose-dependent effects in the Hp ($F_{(2, 15)}$=28.12; Fig. 4B) and Ctx ($F_{(2, 15)}$=79.37, p<0.0001), where the 3xTg-AD 500 mg/kg mice exhibited higher levels than the 3xTg-AD 50 mg/kg mice (Hp p=0.0046, Ctx p<0.0001; Fig. 4B), and 3xTg-AD 50 mg/kg mice showed higher levels than the 3xTg-AD 0 mg/kg mice (Hp p=0.0073, Ctx p<0.0001). For insoluble pTau Thr 181, we found a significant effect of dose for the Hp ($F_{(2, 15)}$=24.61, p<0.0001; Fig. 4C) and Ctx ($F_{(2, 15)}$=6.600, p=0.0088), where the 3xTg-AD 50 mg/kg group showed higher levels in the Hp compared to the 0 mg/kg (p<0.0001) and 500 mg/

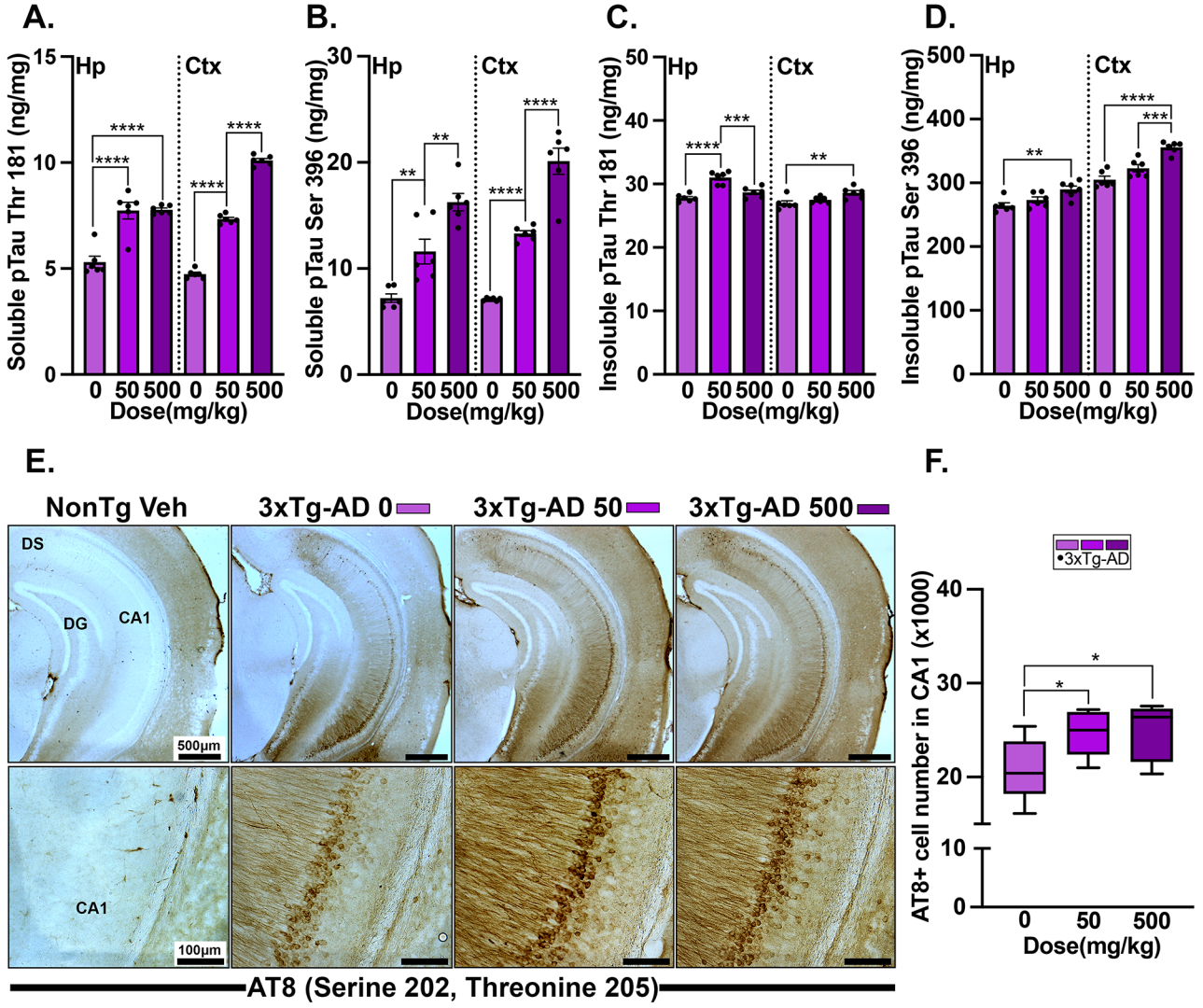

Fig. 4 Glyphosate exposure followed by a recovery period increases phosphorylated pathological tau. (**A**-**D**) Soluble and insoluble fractions of phosphorylated tau at Threonine (Thr) 181 and Serine (Ser) 396 in hippocampal (Hp) and cortex (Ctx) tissue. (**E**, **F**) AT8 (Ser 202/Thr 205) + cell number was significantly elevated in the CA1 region of the Hp of 3xTg-AD 50 mg/kg and 500 mg/kg. *Abbreviations: DS = dorsal subiculum, DG = dentate gyrus, CA1 = cornus ammonis 1.* Bar graphs are means ± SE. For box plots, the center line represents the median value, the limits represent the 25th and 75th percentile, and the whiskers represent the minimum and maximum value of the distribution. Bar graphs are means ± SEM. *p < 0.05, **p < 0.01, ***p < 0.001, ****p < 0.0001

kg ($p=0.0005$) counterparts, and the 3xTg-AD 500 mg/kg had higher levels than the 0 mg/kg ($p=0.0084$) in the Ctx. For insoluble pTau Ser 396, we found a significant effect in the Hp ($F_{(2, 15)}=7.025$, $p=0.0070$; Fig. 4D), where the 3xTg-AD 500 mg/kg mice showed higher levels than the 3xTg-AD 0 mg/kg group ($p=0.0065$). In the Ctx, we found a significant effect ($F_{(2, 15)}=26.26$, $p<0.0001$), where the 3xTg-AD 500 mg/kg showed higher levels than the 3xTg-AD 50 mg/kg ($p=0.0010$) and 3xTg-AD 0 mg/kg ($p<0.0001$) groups. Lastly, we stained tissue against AT8 ($n=6$/group), which is associated with intraneuronal tau filaments [43], and found significantly higher AT8+cells in CA1 of the Hp of 3xTg-AD 50 mg/kg and 500 mg/kg compared to the 0 mg/kg ($t_{(6)}=2.462$, $p=0.049$; Fig. 4E, F). These results are the first demonstration that glyphosate exposure increases hyperphosphorylated tau. Collectively, these data demonstrate that early exposure to glyphosate increases AD-like neuropathology in 3xTg-AD mice.

3xTg-AD glyphosate-exposed mice exhibit significantly increased cytokines and chemokine levels in blood plasma

Elevation of cytokines (pro- and anti-inflammatory) and chemokines (secreted proteins within the cytokine family that induce cell migration) is indicative of inflammation [52]. Previous work shows that glyphosate exposure increases the levels of pro-inflammatory cytokines in circulating blood, liver, and the brain, such as TNF-α, which has been linked to neurotoxicity, cell death and disorders such as AD [6, 53, 54]. To determine whether early glyphosate exposure produced long-lasting peripheral inflammatory changes, we performed a 23-plex cytokine/chemokine panel of peripheral blood plasma of mice ($n=7$–9 NonTg; $n=3$–7/ 3xTg-AD). Levels of cytokines and chemokines were non-detectable in NonTg blood plasma. However, we did find a significant genotype by dose interaction for all 23 markers, indicating significant elevations in the 3xTg-AD-dosed mice (Fig. 5A). Figure 5A highlights the significant elevations across all 23 markers, suggesting that despite a 6-month recovery, glyphosate exposure induced long-lasting increases in

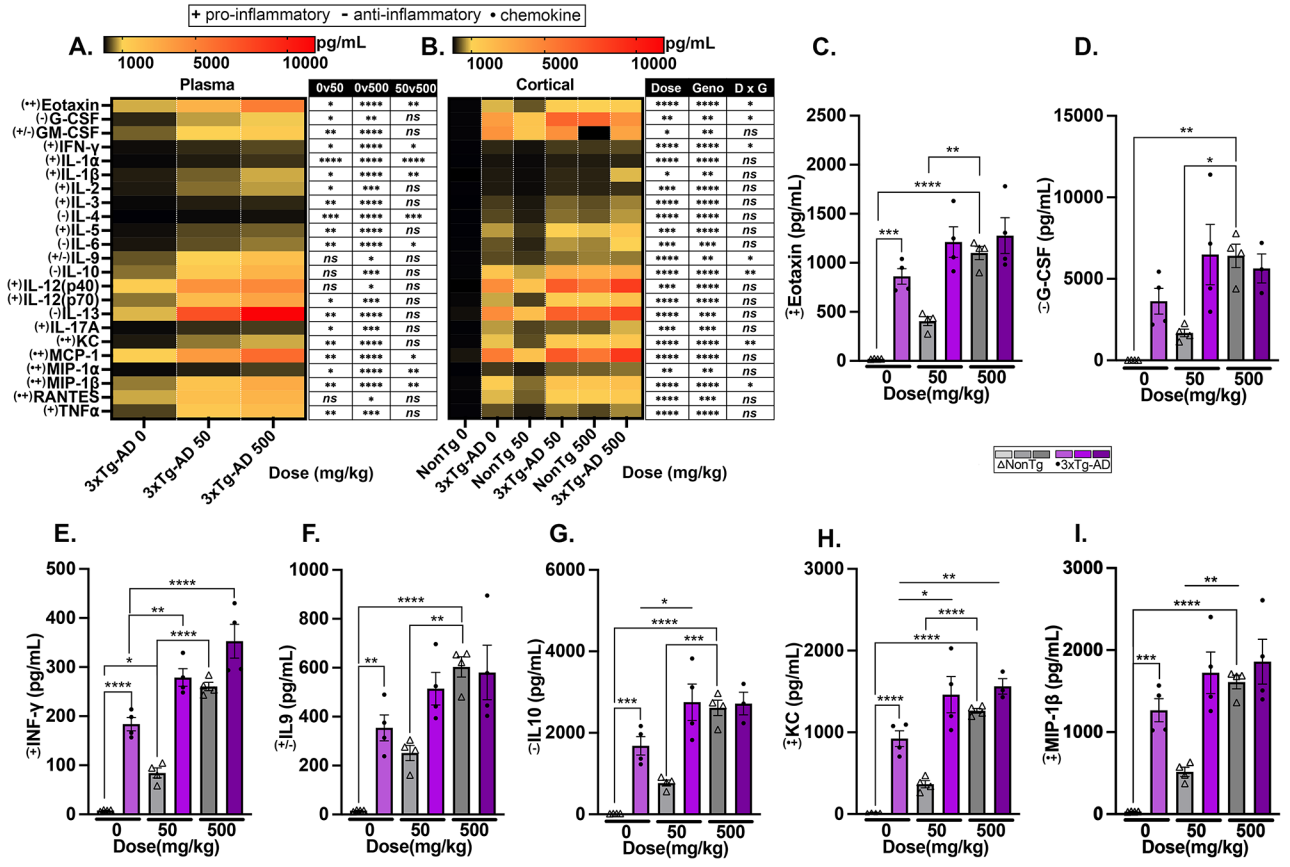

Fig. 5 Glyphosate exposure followed by a recovery period increases cytokine and chemokine levels in blood plasma in 3xTg-AD mice, and in both NonTg and 3xTg-AD cortical tissue. (**A**, **B**) Heat map illustrating significant increases in cytokine and chemokines in blood plasma in 3xTg-AD mice (values were below detection levels in NonTg mice), and in cortical tissue homogenates of both NonTg and 3xTg-AD mice. (**C**-**I**) Significant genotype by dose interactions were graphed to illustrate differences across the two variables. Bar graphs are means ± SEM. *$p<0.05$, **$p<0.01$, ***$p<0.001$, ****$p<0.0001$

peripheral inflammatory molecules that may have contributed to the increased mortality in 3xTg-AD mice.

Glyphosate-exposed NonTg and 3xTg-AD mice show increases in cytokines and chemokine levels in the Ctx

Neuroinflammation is a critical pathophysiological process implicated in the development of neurodegenerative diseases [23, 24]. To determine whether early glyphosate exposure produced long-lasting inflammatory changes in the brain, we performed the 23-plex panel using cortical brain homogenates of a subgroup of mice (n=4/group). We found significant main effects of genotype and dose for all 23 markers, with 3xTg-AD showing higher levels than NonTg and the 50 mg/kg and 500 mg/kg showing higher levels than 0 mg/kg groups (Fig. 5B). We also found a significant genotype by dose interactions for seven pro-inflammatory cytokines. For Eotaxin (C-C motif ligand 1, CCL1), an immune marker of accelerated aging and neurodegeneration [55], we found a significant genotype by dose interaction ($F_{(2,\ 18)}$=5.987, p=0.0102; Fig. 5C), where NonTg 500 mg/kg mice showed higher levels than 50 mg/kg (p=0.0017) and 0 mg/kg (p<0.0001) NonTg counterparts. For granulocyte-colony stimulating factor (G-CSF), a growth factor that promotes neuroprotective effects and is dysregulated in AD [56], we found a significant genotype by dose interaction ($F_{(2,\ 17)}$=4.416, p=0.0286; Fig. 5D), where the NonTg 500 mg/kg mice showed higher levels than 50 mg/kg (p=0.0170) and 0 mg/kg (0.0012) NonTg counterparts. For interferon-gamma (IFN-γ), a pro-inflammatory cytokine that activates macrophages and is an inducer of class II major histocompatibility complex (MHC), whose presence in the brain has been associated with breach of the BBB and neurodegeneration [57, 58], we found a significant genotype by dose interaction ($F_{(2,\ 18)}$=4.792, p=0.0215; Fig. 5E). Post hoc analysis revealed a significant dose-dependent effect in the NonTg mice, where the 500 mg/kg had higher levels than the 50 mg/kg group (p<0.0001), and the 50 mg/kg group had higher levels than the 0 mg/kg groups (p=0.0455). In the 3xTg-AD mice, we found a significant elevation in the 50 mg/kg mice compared to the 0 mg/kg group (p=0.0087). For interleukin (IL) -9, a pro-inflammatory cytokine that promotes cell proliferation, prevents apoptosis, and is associated with progression of mild cognitive impairment (MCI) to AD [59], we found a significant genotype by dose interaction ($F_{(2,\ 18)}$=4.872, p=0.0204; Fig. 5F). Post hoc analysis revealed that NonTg 500 mg/kg had significantly higher levels than both the NonTg 50 mg/kg group (p=0.0049) and 0 mg/kg group (p<0.0001). For IL-10, an anti-inflammatory cytokine that limits immune response to maintain homeostasis and is elevated in AD [60, 61], a significant genotype by dose interaction revealed ($F_{(2,17)}$=7.745, p=0.0041; Fig. 5G) elevations in the NonTg 500 mg/kg group compared to the 50 mg/kg (p=0.0003) and 0 mg/kg NonTg groups (p<0.0001). 3xTg-AD 50 mg/kg dose mice showed significant elevations compared to the 0 mg/kg counterparts (p=0.0441). The chemokine keratinocyte-derived cytokine (KC), also known as CXCL1, is upregulated in response to inflammation, however it has been shown to increase tau hyperphosphorylation, a pathogenic mechanism observed in AD [62]. We found a significant genotype by dose interaction ($F_{(2,\ 17)}$=6.723, p=0.0071; Fig. 5H), where NonTg 500 mg/kg showed an increase compared to the 50 mg/kg (p=0.0001) and 0 mg/kg (p<0.0001) NonTg groups. In 3xTg-AD mice, we found a significant increase in the 50 mg/kg (p=0.0182) and 500 mg/kg (p=0.0085) compared to the 0 mg/kg group. Lastly, we measured levels of macrophage inflammatory protein (MIP) 1-β, also known as CCL4, which has been shown to disrupt neurovascular endothelium and increase Aβ [63, 64]. We found a significant genotype by dose interaction ($F_{(2,\ 18)}$=5.598, p=0.0129; Fig. 5I), where the NonTg 500 mg/kg group had significantly higher levels than the 50 mg/kg (p=0.0015) and 0 mg/kg (p<0.0001) NonTg counterparts. Collectively, these results highlight that even after a 6-month recovery, inflammatory cytokines and chemokines are elevated in cortical tissue of both NonTg and 3xTg-AD mice, and may contribute to the progression of AD-pathogenesis.

Discussion

In the present study, we sought to determine whether glyphosate and aminomethylphosphonic acid would persist in mice following a 6-month recovery period, and whether this exposure/recovery paradigm would alter neuroinflammation and AD pathology. Aminomethylphosphonic acid was detectable in brain tissue of mice dosed with glyphosate, with higher-dosed animals exhibiting higher accumulation. Additionally, we found a significant increase in soluble and insoluble fractions of Aβ, $Aβ_{42}$ plaque load and plaque size, and pTau at Thr 181 and Ser 396 in Hp and Ctx brain tissue from glyphosate-exposed mice, highlighting an exacerbation of hallmark AD-like proteinopathies. We also observed elevations in AT8 in the Hp, collectively demonstrating increased tau pathogenesis with glyphosate exposure for the first time. Notably, we found elevations in pro- and anti-inflammatory cytokines and chemokines in blood plasma of 3xTg-AD mice and in both 3xTg-AD and NonTg mice cortical brain tissue despite recovery. This is significant as prolonged inflammation has been shown to affect the progression of AD pathology and increase the likelihood of developing a neurodegenerative disease [52, 65–67]. Thigmotaxia - a behavior where animals spend more time close to walls and one which is classified as an anxiety-like behavior [68] - was significantly elevated in 3xTg-AD glyphosate-exposed mice. Taken together, our results are

the first to show increased AD-like pathology and elevated inflammation in the peripheral blood and brains of glyphosate-exposed mice, with presence of aminomethylphosphonic acid months after glyphosate exposure (Fig. 6).

Mice dosed with glyphosate did not show significant weight loss during the dosing and recovery periods of the study, consistent with previous reports in glyphosate exposed rodents [18, 69, 70]. However, a higher percentage of 3xTg-AD mice died prematurely during the dosing and recovery period, suggesting that underlying health issues in the AD model may be exacerbated by glyphosate exposure. For example, 3xTg-AD mice exhibit impaired glucose metabolism and insulin resistance [29], as well as an increased susceptibility to high inflammatory responses following acute infection when compared to NonTg mice [71]. Here, we found that elevated peripheral cytokine and chemokine levels were present in 3xTg-AD mice months after glyphosate recovery, but not in NonTg mice. While we did not assess glucose levels or organ pathologies beyond peripheral blood and brain tissue, it is possible that the increased peripheral blood cytokine and chemokine levels observed in 3xTg-AD mice contributed to an exacerbation of already-present ailments, leading to decreased survival. Previous work in rats has shown that glyphosate exposure disrupted glucose homeostasis and insulin signaling, leading to hepatic inflammation and liver damage – all factors which can lead to type II diabetes [72]. Additionally, work in humans has shown that higher urine glyphosate concentrations are associated with type II diabetes, hypertension, cardiovascular disease, and obesity [73]. Thus, it is tempting to speculate that glyphosate exposure may have increased such metabolic ailments, contributing to premature death in 3xTg-AD mice. Future work is needed to dissect such interactions.

Aminomethylphosphonic acid shows similar toxicity to glyphosate [74], and previous work has identified that measurable aminomethylphosphonic acid in humans is associated with oxidative damage and adverse metabolic outcomes [54, 75]. Surprisingly, we found that aminomethylphosphonic acid was present in brain tissue of both 3xTg-AD and NonTg mice months after glyphosate dosing. The mechanism by which aminomethylphosphonic acid entered and was present in cortical brain tissue after glyphosate exposure remains unknown. The

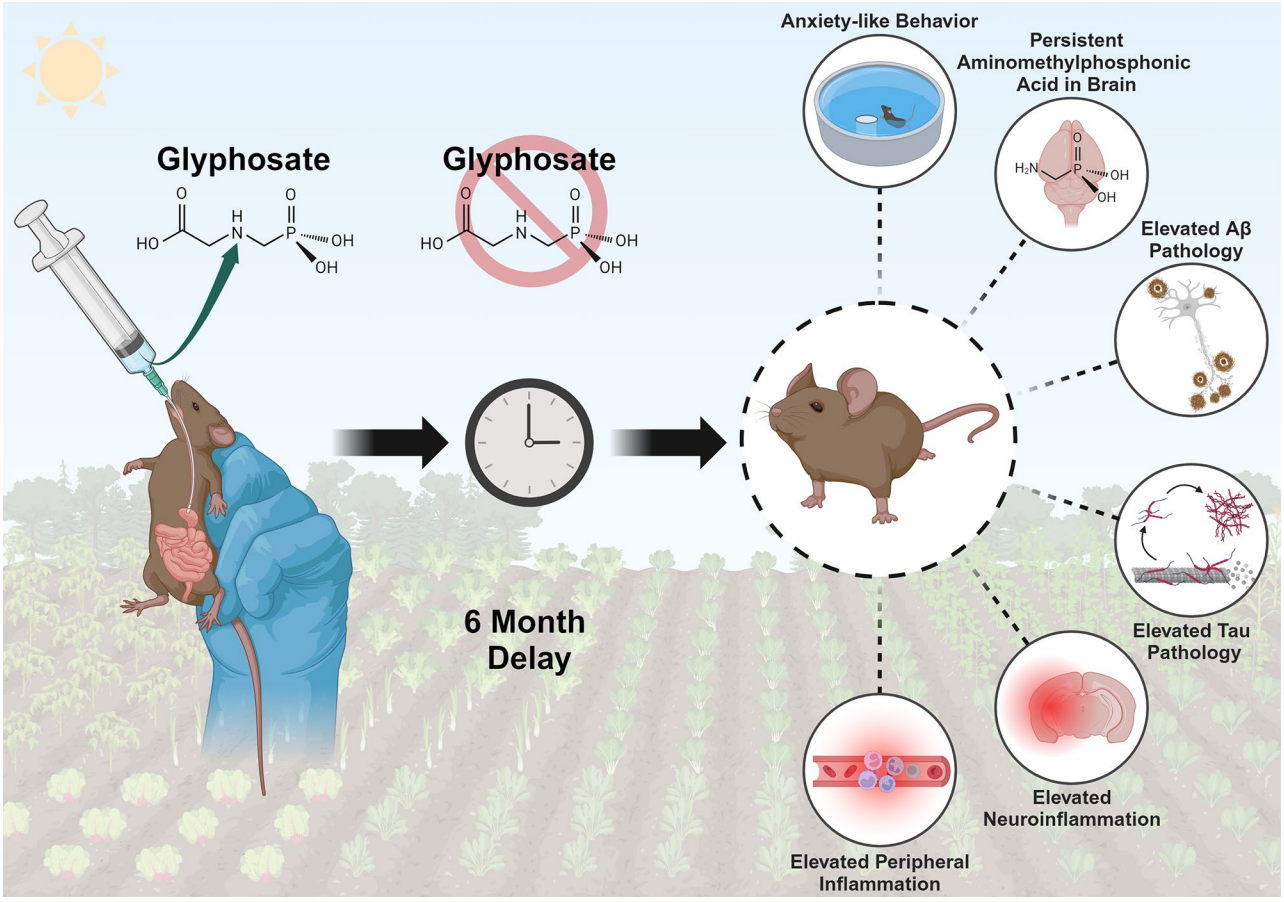

Fig. 6 Graphical abstract of our major findings highlighting that exposure to glyphosate followed by a significant recovery period was capable of eliciting long-lasting pathological consequences

most probable hypothesis is that, during the dosing regimen, glyphosate was metabolized into aminomethylphosphonic acid by the gut microbiome. This is supported by evidence that the gut microbiome of rodents and humans contain microbes, such as *Lactobacilli* and *Bacteroides*, with a shikimate pathway. Most of the bacteria in the human gut microbiome contain the class of 5-enolpyruvylshikimate 3-phosphate synthase enzymes rendering them sensitive to inhibition by glyphosate [21, 76]. Subsequently, we hypothesize that aminomethylphosphonic acid crossed the BBB, leading to its detection in cortical tissue months after glyphosate exposure. This is supported by work showing that aminomethylphosphonic acid crosses the BBB in an in vitro model [28]. Furthermore, 3xTg-AD mice show microvascular degeneration that is evident prior to plaque onset and gets worse with age [77], perhaps due to an impaired capacity to maintain BBB integrity which has been shown using in vitro BBB models derived from 3xTg-AD astrocytes [78]. Notably, patients with acute glyphosate poisoning show increases in serum s100β [79], which indicates disrupted BBB permeability [80]. Moreover, increased and prolonged neuro- and peripheral inflammation can weaken the BBB [81, 82]. Thus, individuals who exhibit increased inflammation and are vulnerable to disruptions in BBB integrity may be at an increased risk of suffering the deleterious effects due to the ability of glyphosate to infiltrate the brain. A second possibility is that glyphosate crossed through the BBB, as we have demonstrated previously [6], and was subsequently metabolized there. However, this seems less likely as, to our knowledge, there is no evidence that the brain can metabolize glyphosate.

Most glyphosate and aminomethylphosphonic acid studies associate urinary levels of exposure with disease outcomes. No recent studies have investigated bioaccumulation of glyphosate and aminomethylphosphonic acid in tissues as most assume near-complete clearance through standard mammalian excretion routes [83, 84]. Our study is the first to report accumulation of aminomethylphosphonic acid in tissue after a significant recovery period, more specifically in brains of rodents. This finding highlights the need to investigate aminomethylphosphonic acid clearance in tissues and warrants additional studies to determine its molecular interactions and long-term effects on health. Notably, in plants, accumulated aminomethylphosphonic acid has been shown to chelate and sequester bi- and tri-valent metal cations such as Ca^{2+}, Zn^{2+}, Cu^{2+}, Mg^{2+}, and Al^{3+} [85]. In humans, heavy metals have been thought to play a role in the pathophysiological process leading to AD [86, 87], suggesting that aminomethylphosphonic acid could chelate select heavy metals in the brain, leading to AD-associated neurotoxicity.

We found long-lasting elevations of various cytokines and chemokines, highlighting neuroinflammation induced by glyphosate exposure in both 3xTg-AD and NonTg mice, consistent with previously-published work showing that glyphosate exposure resulted in increased TNF-α [6]. The increases in several pro- and anti-inflammatory cytokines in the brain suggest that aminomethylphosphonic acid may contribute to dysregulated neuroimmune function months after exposure, although future work is necessary to determine the mechanism of such interaction. Another possibility is that glyphosate exposure may have initiated chronic release of cytokines and chemokines that continues for months. While inflammation is a necessary part of the body's immune response, prolonged neuroinflammation can be detrimental to the body and brain (reviewed in [88]). Glyphosate has been shown to increase peripheral inflammation: in vitro work demonstrated that exposure of T-cells to glyphosate and its metabolites can directly lead to increased cytokine production [89] and increased reactive oxygen species [90]. Additionally, in mice, short-term administration of glyphosate led to peripheral immune activation and inflammation [91]. 3xTg-AD mice already show heightened peripheral pro-inflammatory responses to infection, with neuroinflammation increasing even when an infection is in the periphery [71]. Given that glyphosate dosing increased peripheral inflammation in our 3xTg-AD mice, despite an absence of circulating glyphosate or aminomethylphosphonic acid, there are three intriguing possibilities to explain the prolonged elevation of peripheral inflammation in the 3xTg-AD mice. Firstly, we did not examine accumulated aminomethylphosphonic acid in other organs; liver and adipose tissue have been shown to cause increased generation of inflammatory cytokines upon glyphosate exposure [92]. Thus, if glyphosate or its metabolites remained in the other organs, it may be continuing to drive chronic peripheral inflammation in the 3xTg-AD mice. Secondly, glyphosate exposure can alter the expression of chromatin remodeling genes in immune cells in vitro [93], which could have led to sustained peripheral inflammation via epigenetic mechanisms. Finally, given the BBB disruptions in the 3xTg-AD strain, it is possible that cytokines generated in the brain from the remaining aminomethylphosphonic acid could have crossed into peripheral circulation, exacerbating inflammatory signaling.

The significant elevations in both pro- and anti-inflammatory cytokines found in the brains of both AD and NonTg mice may have further implications for cognitive dysfunction related to glyphosate exposure. For example, increased levels of plasma Eotaxin and MCP (monocyte chemoattractant protein)-1 are associated with worsening memory in aging adults and those with neurodegenerative diseases, such as AD [94]. We found

that both Eotaxin and MCP-1 were significantly elevated in plasma and brain of our glyphosate dosed-mice. Additionally, IFN-γ - a cytokine significantly increased in glyphosate-dosed mice - can induce a neurotoxic phenotype in microglia; during disease states, this can further neuroinflammation and result in oxidative stress, and eventual cell death [95, 96]. Increased IFN-γ expression also impairs adult hippocampal neurogenesis, which can consequently affect learning and memory [96]. Twelve interleukins (IL), a class of cytokines with a wide range of functions centered around the immune response, were significantly increased in cortical tissue of all mice given glyphosate: IL-1α, IL-1β, IL-2, -3, -4, -5, -6, -9, -10, -12(p40), -12(p70), -13, and -17. Of these twelve, IL-4, IL-10, and IL-13, are anti-inflammatory cytokines, but prior research has shown that elevated IL-4 and IL-10 can increase Aβ plaque burden [97, 98]. There are mixed conclusions about the implications of individual cytokines on AD; however, the consensus is that the immune response is comprised of a delicate balance of pro- and anti-inflammatory cytokines which is ultimately disrupted in AD and contributes to progression of neuropathology [99, 100]. Since we found that exposure to glyphosate promoted an imbalance of pro- and anti-inflammatory cytokine and chemokine levels in the brain and periphery of 3xTg-AD mice, this may pose profound implications for glyphosate exposure as a risk factor for AD.

Whether through disruption of neuroinflammation, or a more direct mechanism, glyphosate exposure increased Aβ and tau pathology in our 3xTg-AD mice. Notably, amyloidogenic APP processing and tau hyperphosphorylation is worsened with increased cytokine levels [101–103], which was observed in the glyphosate-dosed mice, and we found increased APP processing of C-terminal fragments C99 through elevations in BACE-1. Our group has previously shown that exposing primary neurons from a mouse model of APP overexpression to glyphosate in vitro increased $A\beta_{40}$ and $_{42}$ levels [6]. Additionally, work has shown that N2a cells overexpressing the APP Swedish mutation, then exposed to a combination of IFN-γ plus TNF-α, and IFN-γ plus IL-1β, lead to a significant increase in BACE-1 expression and mRNA levels [104]. TNF-α, IFN-γ, and IL-1β were all significantly elevated in both blood plasma and cortical tissue from mice exposed to glyphosate, suggesting these increased inflammatory cytokines could be directly affecting the expression of BACE-1. Also, the BACE-1 gene contains a lymphokine response element within its promoter sequence, making it possible for lymphokines to alter the transcription of BACE-1 [104]. Lymphokines include IL-2, -3, -4, -5, and −6, cytokines which we found to be elevated in mice exposed to glyphosate, offering transcriptional changes as a mechanism for increased BACE-1 expression. We suggest that the accumulation of aminomethylphosphonic acid that remained in the brain during recovery, or glyphosate that may have crossed into the brain during exposure, lead to increased cytokine levels, which increased the expression of BACE-1, increasing amyloidogenic processing and ultimately elevations in amyloidosis. Elevated neuroinflammation may have also contributed to increased tau pathology, as previous work has demonstrated that infection-induced chronic inflammation worsens pathological tau by increasing glycogen synthase kinase-3β activity (GSK-3β), a kinase that can aberrantly contribute to tau hyperphosphorylation [105]. Lastly, exposure to glyphosate and aminomethylphsophonic acid has been linked to transcriptomic changes [6], oxidative damage [54, 75], and disruptions in DNA repair mechanisms [106]. DNA repair mechanisms are critical to safeguard the integrity of a cell's genetic information. Impaired repair of oxidative DNA damage has been linked to the development and progression of AD [107, 108]. Thus, we speculate that early glyphosate exposure and prolonged aminomethylphosphonic acid in the brain may have contributed to dysregulated DNA damage repair mechanisms, exacerbating AD-like pathology.

We found that glyphosate-exposed 3xTg-AD mice performed similarly in tasks assessing learning and memory compared to the 3xTg-AD 0 mg/kg dosed mice. However, increased thigmotaxia was observed in glyphosate-exposed 3xTg-AD mice. 3xTg-AD mice exhibit significantly increased thigmotaxia in the MWM compared to NonTg mice [109, 110], and aged females, in particular, exhibit a higher level of fear and anxiety demonstrated by increased restlessness, startle responses, and freezing behaviors [111]. A heightened anxiety phenotype is consistent with reports showing that glyphosate exposure increases anxiety-like behaviors in rodents [12, 36, 112]. In humans, amygdalar atrophy and Aβ accumulation are observed early in AD [3, 113, 114], with patients often experiencing anxiety symptoms [114, 115]. 3xTg-AD mice show accumulation of intraneuronal Aβ in the amygdala [116], which has been associated with amygdala-dependent emotional responses and heightened anxiety-like behavior [35, 111, 117]. Additionally, neuroinflammation in the amygdala has been demonstrated to contribute to anxiety-like behavior [118, 119], which in the current study may have extended to the amygdala of 3xTg-AD glyphosate-exposed mice that are already susceptible to anxiety, contributing to increased thigmotaxia in the MWM. Finally, thigmotaxia can be used as a technique when mice cannot locate a hidden platform due to spatial memory impairments [120]. The question remains if the behavioral differences are due specifically to the exposure to glyphosate and accumulated aminomethylphosphonic acid in the brain, the increased AD pathology and neuroinflammation, which

may have extended to the amygdala, or a combination of both in 3xTg-AD mice, which will be examined in future work.

Conclusion

In conclusion, glyphosate exposure resulted in premature death, accelerated AD-like pathology and subsequent anxiety-like behaviors in 3xTg-AD mice, and neuroinflammation in both NonTg and AD mice, despite months of recovery (Fig. 6). The multifactorial consequences of glyphosate exposure are increasingly concerning given the ubiquity of its use. The fact that we found accumulation of aminomethylphosphonic acid in brains following recovery from exposure is particularly concerning, especially given its association with increased neuroinflammation in both NonTg and AD mice. As glyphosate use continues to rise, more research is needed to elucidate the impact of this herbicide and its metabolites on the human brain and their potential contribution toward the increased prevalence of neurodegenerative disorders.

Data Availability

The data that supporting the findings of this study will be made available by the corresponding authors upon reasonable request.

Abbreviations

AD	Alzheimer's Disease
US	United States
Aβ	Amyloid Beta
NFT	Neurofibrillary tau tangles
EPA	Environmental Protection Agency
BBB	Blood brain barrier
TNF-α	Tumor necrosis factor-α
NonTg	Non-transgenic
NOAEL	No observable adverse effect limit
MWM	Morris Water Maze
EDTA	Ethylenediaminetetraacetic acid
MWCO	Molecular weight cut-off
LC-MS/MS	Liquid chromatography/tandem mass spectrometry
RSD	Relative standard deviation
LOD	Lower limit of quantitation
LOQ	Limit of quantitation
ELISA	Enzyme-linked immunosorbent assay
PBS	Phosphate buffered saline
Hp	Hippocampus
Ctx	Cortex
FL-APP	Full-length amyloid precursor protein
GAPDH	Glyceraldehyde 3-phosphate dehydrogenase
BACE-1	Beta-secretase 1
C99	99 amino acid C-terminal fragment of amyloid precursor protein
$Aβ_{40}$, $Aβ_{42}$	Amyloid Beta, peptide lengths 40 and 42
Thr 181	Threonine 181
Ser 396	Serine 396
pTau	Phosphorylated tau
UHPLC	Ultra high-pressure liquid chromatography
LC-MRM	Liquid chromatography with multiple reaction monitoring
AT8	Tau phosphorylated at serine 202 and threonine 205
CA1	Cornu ammonis 1
ANOVA	Analysis of variance
UPLC-MS	Ultra-performance liquid chromatography- mass spectrometry
APP	Amyloid Precursor Protein
G-CSF	Granulocyte-colony stimulating factor
IFN-γ	Interferon-gamma
MHC	Major histocompatibility complex
IL	Interleukin
KC	Keratinocyte-derived cytokine
MCI	Mild cognitive impairment
KC/CXCL1	Chemokine ligand 1
MIP1-β	Macrophage inflammatory protein 1-β
MCP-1	Monocyte chemoattractant protein 1

Supplementary Information

The online version contains supplementary material available at https://doi.org/10.1186/s12974-024-03290-6.

Supplementary Material 1: Supplementary Fig. 1. Calibration curves of (A) glyphosate and (B) aminomethylphosphonic acid over a concentration range of 0–3 ng/mL in plasma, x-axis and y-axis represent variable concentration of glyphosate and aminomethylphosphonic acid, and area ratio of variable concentration of glyphosate or aminomethylphosphonic acid to their internal standards ($^{13}C^{15}N$ Glyphosate, or $^{13}C^{15}N$ aminomethylphosphonic acid).

Supplementary Material 2: Supplementary Fig. 2. Calibration curves of (A) glyphosate and (B) aminomethylphosphonic acid over a concentration range of 0–60 ng/g in brain. x-axis and y-axis represent variable concentration of glyphosate and aminomethylphosphonic acid, and area ratio of variable concentration of glyphosate or aminomethylphosphonic acid to their internal standards ($^{13}C^{15}N$ Glyphosate, or $^{13}C^{15}N$ aminomethylphosphonic acid) respectively

Supplementary Material 3: Uncropped westernblot of Ctx full length APP (6e10)

Supplementary Material 4: Uncropped westernblot of Ctx GAPDH

Supplementary Material 5: Uncropped westerblot of Hp GAPDH

Supplementary Material 6: Uncropped westernblot of Hp full length APP (6e10)

Acknowledgements

Figure 6 was created in BioRender. Tallino, S. (2024) https://biorender.com/e40j043

Author contributions

SKB: Animal dosing, behavioral testing, tissue processing, wrote and edited manuscript. WW: Biochemical analysis, statistical analysis, wrote and edited manuscript. RS: Assistance with UPLC measurements, edited the manuscript. KVP: UPLC measurements, edited the manuscript. ST: Behavior testing, statistical analysis, wrote and edited the manuscript. JJ: Behavior testing, histology, stereology, wrote and edited the manuscript. HL: Histology, edited the manuscript. JT: Histology, western blots, edited the manuscript. PP: Funding, experimental design, statistical analysis, wrote and edited the manuscript. RV: Funding, experimental design, statistical analysis, wrote and edited the manuscript. All authors read and approved the final manuscript.

Funding

This work was supported by grants to Ramon Velazquez from the ASU Edson Initiative Seed grant program and the National Institute on Aging (R01 AG059627) and (R01 AG062500). This reported research includes work performed in the Integrated Mass Spectrometry Shared Resource supported by the National Cancer Institute of the National Institutes of Health under grant number P30CA033572.

Data availability

No datasets were generated or analysed during the current study.

Ethics approval and consent to participate

Not applicable.

Consent for publication
Not applicable.

Competing interests
The authors declare no competing interests.

Author details
[1]Arizona State University-Banner Neurodegenerative Disease Research Center at the Biodesign Institute, Arizona State University, Tempe, AZ, USA
[2]School of Life Sciences, Arizona State University, Tempe, AZ, USA
[3]Integrated Mass Spectrometry Shared Resources, City of Hope Comprehensive Cancer Center, Duarte, CA, USA
[4]Cancer & Cell Biology Division, Translational Genomics Research Institute, Phoenix, AZ, USA

Received: 30 August 2024 / Accepted: 7 November 2024
Published online: 04 December 2024

References

1. 2024 Alzheimer's disease facts and figures. Alzheimers Dement J Alzheimers Assoc. 2024;20:3708–821.
2. Bakota L, Brandt R. Tau Biology and Tau-Directed therapies for Alzheimer's Disease. Drugs. 2016;76:301–13.
3. Braak H, Braak E. Neuropathological stageing of Alzheimer-related changes. Acta Neuropathol (Berl). 1991;82:239–59.
4. Vasefi M, Ghaboolian-Zare E, Abedelwahab H, Osu A. Environmental toxins and Alzheimer's disease progression. Neurochem Int. 2020;141:104852.
5. Rahman MA, Rahman MS, Uddin MJ, Mamum-Or-Rashid ANM, Pang M-G, Rhim H. Emerging risk of environmental factors: insight mechanisms of Alzheimer's diseases. Environ Sci Pollut Res. 2020;27:44659–72.
6. Winstone JK, Pathak KV, Winslow W, Piras IS, White J, Sharma R, et al. Glyphosate infiltrates the brain and increases pro-inflammatory cytokine TNFα: implications for neurodegenerative disorders. J Neuroinflammation. 2022;19:193.
7. Benbrook CM. Trends in glyphosate herbicide use in the United States and globally. Environ Sci Eur. 2016;28:3.
8. USGS NAWQA. The Pesticide National Synthesis Project [Internet]. [cited 2024 Feb 21]. https://water.usgs.gov/nawqa/pnsp/usage/maps/
9. Funke T, Han H, Healy-Fried ML, Fischer M, Schönbrunn E. Molecular basis for the herbicide resistance of Roundup Ready crops. Proc Natl Acad Sci U S A. 2006;103:13010–5.
10. Martins-Gomes C, Silva TL, Andreani T, Silva AM. Glyphosate vs. glyphosate-based herbicides exposure: a review on their toxicity. J Xenobiotics. 2022;12:21–40.
11. Agostini LP, Dettogni RS, Dos Reis RS, Stur E, Dos Santos EVW, Ventorim DP, et al. Effects of glyphosate exposure on human health: insights from epidemiological and in vitro studies. Sci Total Environ. 2020;705:135808.
12. Aitbali Y, Ba-M'hamed S, Elhidar N, Nafis A, Soraa N, Bennis M. Glyphosate based- herbicide exposure affects gut microbiota, anxiety and depression-like behaviors in mice. Neurotoxicol Teratol. 2018;67:44–9.
13. Izumi Y, O'Dell KA, Zorumski CF. The herbicide glyphosate inhibits hippocampal long-term potentiation and learning through activation of pro-inflammatory signaling. Res Sq. 2023;rs.3.rs-2883114.
14. Ren J, Yu Y, Wang Y, Dong Y, Shen X. Association between urinary glyphosate exposure and cognitive impairment in older adults from NHANES 2013–2014. J Alzheimers Dis JAD. 2024;97:609–20.
15. Yang A-M, Chu P-L, Wang C, Lin C-Y. Association between urinary glyphosate levels and serum neurofilament light chain in a representative sample of US adults: NHANES 2013–2014. J Expo Sci Environ Epidemiol. 2024;34:287–93.
16. Lehmann S, Schraen-Maschke S, Vidal J-S, Blanc F, Paquet C, Allinquant B, et al. Blood neurofilament levels predict Cognitive decline across the Alzheimer's Disease Continuum. Int J Mol Sci. 2023;24:17361.
17. Williams GM, Kroes R, Munro IC. Safety evaluation and risk assessment of the herbicide Roundup and its active ingredient, glyphosate, for humans. Regul Toxicol Pharmacol RTP. 2000;31:117–65.
18. Panzacchi S, Mandrioli D, Manservisi F, Bua L, Falcioni L, Spinaci M, et al. The Ramazzini Institute 13-week study on glyphosate-based herbicides at human-equivalent dose in Sprague Dawley rats: study design and first in-life endpoints evaluation. Environ Health. 2018;17:52.
19. Herrmann KM, Weaver LM. THE SHIKIMATE PATHWAY. Annu Rev Plant Physiol Plant Mol Biol. 1999;50:473–503.
20. Rueda-Ruzafa L, Cruz F, Roman P, Cardona D. Gut microbiota and neurological effects of glyphosate. Neurotoxicology. 2019;75:1–8.
21. Mesnage R, Antoniou MN. Computational modelling provides insight into the effects of glyphosate on the shikimate pathway in the human gut microbiome. Curr Res Toxicol. 2020;1:25–33.
22. Kumar A, Editorial. Neuroinflammation and Cognition. Front Aging Neurosci. 2018;10:413.
23. Guzman-Martinez L, Maccioni RB, Andrade V, Navarrete LP, Pastor MG, Ramos-Escobar N. Neuroinflammation as a common feature of neurodegenerative disorders. Front Pharmacol. 2019;10:1008.
24. CHEN W-W ZHANGX, HUANG W-J. Role of neuroinflammation in neurodegenerative diseases (review). Mol Med Rep. 2016;13:3391–6.
25. Gerona RR, Reiter JL, Zakharevich I, Proctor C, Ying J, Mesnage R, et al. Glyphosate exposure in early pregnancy and reduced fetal growth: a prospective observational study of high-risk pregnancies. Environ Health Glob Access Sci Source. 2022;21:95.
26. Cattani D, Struyf N, Steffensen V, Bergquist J, Zamoner A, Brittebo E, et al. Perinatal exposure to a glyphosate-based herbicide causes dysregulation of dynorphins and an increase of neural precursor cells in the brain of adult male rats. Toxicology. 2021;461:152922.
27. Cattani D, Pierozan P, Zamoner A, Brittebo E, Karlsson O. Long-Term effects of Perinatal exposure to a glyphosate-based herbicide on melatonin levels and oxidative brain damage in adult male rats. Antioxid Basel Switz. 2023;12:1825.
28. Martinez A, Al-Ahmad AJ. Effects of glyphosate and aminomethylphosphonic acid on an isogeneic model of the human blood-brain barrier. Toxicol Lett. 2019;304:39–49.
29. Velazquez R, Tran A, Ishimwe E, Denner L, Dave N, Oddo S, et al. Central insulin dysregulation and energy dyshomeostasis in two mouse models of Alzheimer's disease. Neurobiol Aging. 2017;58:1–13.
30. Winslow W, McDonough I, Tallino S, Decker A, Vural AS, Velazquez R. IntelliCage Automated behavioral phenotyping reveals Behavior deficits in the 3xTg-AD mouse model of Alzheimer's Disease Associated with Brain Weight. Front Aging Neurosci. 2021;13:720214.
31. Velazquez R, Meechoovet B, Ow A, Foley C, Shaw A, Smith B, et al. Chronic Dyrk1 inhibition delays the Onset of AD-Like Pathology in 3xTg-AD mice. Mol Neurobiol. 2019;56:8364–75.
32. Jax Lab. 034830–3xTg-AD Strain Details [Internet]. 2014 [cited 2024 Jun 28]. https://www.jax.org/strain/004807#
33. Belfiore R, Rodin A, Ferreira E, Velazquez R, Branca C, Caccamo A, et al. Temporal and regional progression of Alzheimer's disease-like pathology in 3xTg-AD mice. Aging Cell. 2019;18:e12873.
34. Roda AR, Montoliu-Gaya L, Serra-Mir G, Villegas S. Both Amyloid-β peptide and tau protein are affected by an Anti-Amyloid-β antibody fragment in Elderly 3xTg-AD mice. Int J Mol Sci. 2020;21:6630.
35. Roda AR, Esquerda-Canals G, Martí-Clúa J, Villegas S. Cognitive impairment in the 3xTg-AD mouse model of Alzheimer's Disease is affected by Aβ-ImmunoTherapy and cognitive stimulation. Pharmaceutics. 2020;12:944.
36. Ait Bali Y, Kaikai N-E, Ba-M'hamed S, Sassoè-Pognetto M, Giustetto M, Bennis M. Anxiety and gene expression enhancement in mice exposed to glyphosate-based herbicide. Toxics. 2022;10:226.
37. EPA. Registration Eligibility Decision (RED) Glyphosate. Office of Prevention, Pesticides and Toxic Substances. EPA-738-F-93-011; 1993.
38. Ait Bali Y, Ba-Mhamed S, Bennis M. Behavioral and immunohistochemical study of the effects of Subchronic and Chronic exposure to glyphosate in mice. Front Behav Neurosci. 2017;11:146.
39. Qi L, Dong Y-M, Chao H, Zhao P, Ma S-L, Li G. Glyphosate based-herbicide disrupts energy metabolism and activates inflammatory response through oxidative stress in mice liver. Chemosphere. 2023;315:137751.
40. Mesnage R, Ibragim M, Mandrioli D, Falcioni L, Tibaldi E, Belpoggi F, et al. Comparative toxicogenomics of glyphosate and Roundup herbicides by mammalian stem cell-based genotoxicity assays and molecular profiling in Sprague-Dawley rats. Toxicol Sci off J Soc Toxicol. 2022;186:83–101.
41. Branca C, Shaw DM, Belfiore R, Gokhale V, Shaw AY, Foley C, et al. Dyrk1 inhibition improves Alzheimer's disease-like pathology. Aging Cell. 2017;16:1146–54.
42. Dave N, Judd JM, Decker A, Winslow W, Sarette P, Villarreal Espinosa O, et al. Dietary choline intake is necessary to prevent systems-wide organ pathology and reduce Alzheimer's disease hallmarks. Aging Cell. 2023;22:e13775.
43. Dave N, Vural AS, Piras IS, Winslow W, Surendra L, Winstone JK et al. Identification of retinoblastoma binding protein 7 (Rbbp7) as a mediator against tau

acetylation and subsequent neuronal loss in Alzheimer's disease and related tauopathies. Acta Neuropathol. 2021, 142, 279–294.
44. Velazquez R, Ferreira E, Knowles S, Fux C, Rodin A, Winslow W, et al. Lifelong choline supplementation ameliorates Alzheimer's disease pathology and associated cognitive deficits by attenuating microglia activation. Aging Cell. 2019;18:e13037.
45. Lesseur C, Pirrotte P, Pathak KV, Manservisi F, Mandrioli D, Belpoggi F, et al. Maternal urinary levels of glyphosate during pregnancy and anogenital distance in newborns in a US multicenter pregnancy cohort. Environ Pollut. 2021;280:117002.
46. Jensen PK, Wujcik CE, McGuire MK, McGuire MA. Validation of reliable and selective methods for direct determination of glyphosate and aminomethylphosphonic acid in milk and urine using LC-MS/MS. J Environ Sci Health B. 2016;51:254–9.
47. Christensen A, Pike CJ. Staining and quantification of β-Amyloid Pathology in Transgenic Mouse models of Alzheimer's Disease. Methods Mol Biol Clifton NJ. 2020;2144:211–21.
48. Javonillo DI, Tran KM, Phan J, Hingco E, Kramár EA, da Cunha C, et al. Systematic phenotyping and characterization of the 3xTg-AD mouse model of Alzheimer's Disease. Front Neurosci. 2021;15:785276.
49. Simon P, Dupuis R, Costentin J. Thigmotaxis as an index of anxiety in mice. Influence of dopaminergic transmissions. Behav Brain Res. 1994;61:59–64.
50. Kandalepas PC, Vassar R. The normal and pathologic roles of the Alzheimer's β-secretase, BACE1. Curr Alzheimer Res. 2014;11:441–9.
51. Lin Y, Im H, Diem LT, Ham S. Characterizing the structural and thermodynamic properties of Aβ42 and Aβ40. Biochem Biophys Res Commun. 2019;510:442–8.
52. Sartori AC, Vance DE, Slater LZ, Crowe M. The impact of inflammation on cognitive function in older adults: implications for healthcare practice and research. J Neurosci Nurs J Am Assoc Neurosci Nurses. 2012;44:206–17.
53. Zhao M, Cribbs DH, Anderson AJ, Cummings BJ, Su JH, Wasserman AJ, et al. The induction of the TNFalpha death domain signaling pathway in Alzheimer's disease brain. Neurochem Res. 2003;28:307–18.
54. Eskenazi B, Gunier RB, Rauch S, Kogut K, Perito ER, Mendez X, et al. Association of Lifetime Exposure to Glyphosate and Aminomethylphosphonic Acid (AMPA) with liver inflammation and metabolic syndrome at Young Adulthood: findings from the CHAMACOS Study. Environ Health Perspect. 2023;131:37001.
55. Ivanovska M, Abdi Z, Murdjeva M, Macedo D, Maes A, Maes M. CCL-11 or Eotaxin-1: an Immune marker for Ageing and Accelerated Ageing in Neuro-Psychiatric disorders. Pharm Basel Switz. 2020;13:230.
56. Laske C, Stellos K, Stransky E, Leyhe T, Gawaz M. Decreased plasma levels of granulocyte-colony stimulating factor (G-CSF) in patients with early Alzheimer's disease. J Alzheimers Dis JAD. 2009;17:115–23.
57. Bate C, Kempster S, Last V, Williams A. Interferon-γ increases neuronal death in response to amyloid-β1–42. J Neuroinflammation. 2006;3:7.
58. Corbin-Stein NJ, Childers GM, Webster JM, Zane A, Yang Y-T, Mudium N, et al. IFNγ drives neuroinflammation, demyelination, and neurodegeneration in a mouse model of multiple system atrophy. Acta Neuropathol Commun. 2024;12:11.
59. Contreras JA, Aslanyan V, Albrecht DS, Mack WJ. Alzheimer's Disease Neuroimaging Initiative (ADNI), Pa J. Higher baseline levels of CSF inflammation increase risk of incident mild cognitive impairment and Alzheimer's disease dementia. Alzheimers Dement Amst Neth. 2022;14:e12346.
60. Cisbani G, Koppel A, Knezevic D, Suridjan I, Mizrahi R, Bazinet RP. Peripheral cytokine and fatty acid associations with neuroinflammation in AD and aMCI patients: an exploratory study. Brain Behav Immun. 2020;87:679–88.
61. Iyer SS, Cheng G. Role of interleukin 10 transcriptional regulation in inflammation and autoimmune disease. Crit Rev Immunol. 2012;32:23–63.
62. Xia M, Hyman BT. GROalpha/KC, a chemokine receptor CXCR2 ligand, can be a potent trigger for neuronal ERK1/2 and PI-3 kinase pathways and for tau hyperphosphorylation-a role in Alzheimer's disease? J Neuroimmunol. 2002;122:55–64.
63. Estevao C, Bowers CE, Luo D, Sarker M, Hoeh AE, Frudd K, et al. CCL4 induces inflammatory signalling and barrier disruption in the neurovascular endothelium. Brain Behav Immun - Health. 2021;18:100370.
64. Pulliam L. HIV regulation of amyloid beta production. J Neuroimmune Pharmacol off J Soc NeuroImmune Pharmacol. 2009;4:213–7.
65. Ogunmokun G, Dewanjee S, Chakraborty P, Valupadas C, Chaudhary A, Kolli V, et al. The potential role of cytokines and growth factors in the pathogenesis of Alzheimer's Disease. Cells. 2021;10:2790.
66. Ahmad MA, Kareem O, Khushtar M, Akbar M, Haque MR, Iqubal A, et al. Neuroinflammation: a potential risk for Dementia. Int J Mol Sci. 2022;23:616.
67. Rani V, Verma R, Kumar K, Chawla R. Role of pro-inflammatory cytokines in Alzheimer's disease and neuroprotective effects of pegylated self-assembled nanoscaffolds. Curr Res Pharmacol Drug Discov. 2023;4:100149.
68. Treit D, Fundytus M. Thigmotaxis as a test for anxiolytic activity in rats. Pharmacol Biochem Behav. 1988;31:959–62.
69. Chan P, Mahler J. NTP technical report on the toxicity studies of glyphosate (CAS 1071-83-6) administered in dosed feed to F344/N rats and B6C3F1 mice. Toxic Rep Ser. 1992;16:1–D3.
70. Ojiro R, Okano H, Takahashi Y, Takashima K, Tang Q, Ozawa S, et al. Comparison of the effect of glyphosate and glyphosate-based herbicide on hippocampal neurogenesis after developmental exposure in rats. Toxicology. 2023;483:153369.
71. Montacute R, Foley K, Forman R, Else KJ, Cruickshank SM, Allan SM. Enhanced susceptibility of triple transgenic Alzheimer's disease (3xTg-AD) mice to acute infection. J Neuroinflammation. 2017;14:50.
72. Prasad M, Gatasheh MK, Alshuniaber MA, Krishnamoorthy R, Rajagopal P, Krishnamoorthy K, et al. Impact of glyphosate on the Development of Insulin Resistance in Experimental Diabetic rats: role of NFκB Signalling pathways. Antioxid Basel Switz. 2022;11:2436.
73. Li W, Lei D, Huang G, Tang N, Lu P, Jiang L, et al. Association of glyphosate exposure with multiple adverse outcomes and potential mediators. Chemosphere. 2023;345:140477.
74. 927. Aminomethylphosphonic acid (Pesticide residues in food:1997 evaluations Part II Toxicological & Environmental) [Internet]. [cited 2024 Mar 17]. https://www.inchem.org/documents/jmpr/jmpmono/v097pr04.htm
75. Makris KC, Efthymiou N, Konstantinou C, Anastasi E, Schoeters G, Kolossa-Gehring M, et al. Oxidative stress of glyphosate, AMPA and metabolites of pyrethroids and chlorpyrifos pesticides among primary school children in Cyprus. Environ Res. 2022;212:113316.
76. Mesnage R, Teixeira M, Mandrioli D, Falcioni L, Ducarmon QR, Zwittink RD, et al. Use of Shotgun metagenomics and metabolomics to evaluate the impact of glyphosate or Roundup MON 52276 on the gut microbiota and serum metabolome of Sprague-Dawley rats. Environ Health Perspect. 2021;129:17005.
77. Quintana DD, Anantula Y, Garcia JA, Engler-Chiurazzi EB, Sarkar SN, Corbin DR, et al. Microvascular degeneration occurs before plaque onset and progresses with age in 3xTg AD mice. Neurobiol Aging. 2021;105:115–28.
78. Kriaučiūnaitė K, Kaušylė A, Pajarskienė J, Tunaitis V, Lim D, Verkhratsky A, et al. Immortalised hippocampal astrocytes from 3xTG-AD mice fail to Support BBB Integrity in Vitro: role of Extracellular vesicles in glial-endothelial communication. Cell Mol Neurobiol. 2021;41:551–62.
79. Lee J-W, Choi Y-J, Park S, Gil H-W, Song H-Y, Hong S-Y. Serum S100 protein could predict altered consciousness in glyphosate or glufosinate poisoning patients. Clin Toxicol Phila Pa. 2017;55:357–9.
80. Kanner AA, Marchi N, Fazio V, Mayberg MR, Koltz MT, Siomin V, et al. Serum S100beta: a noninvasive marker of blood-brain barrier function and brain lesions. Cancer. 2003;97:2806–13.
81. Takeda S, Sato N, Ikimura K, Nishino H, Rakugi H, Morishita R. Increased blood-brain barrier vulnerability to systemic inflammation in an Alzheimer disease mouse model. Neurobiol Aging. 2013;34:2064–70.
82. Takata F, Nakagawa S, Matsumoto J, Dohgu S. Blood-brain barrier dysfunction amplifies the development of Neuroinflammation: understanding of Cellular events in Brain Microvascular endothelial cells for Prevention and Treatment of BBB Dysfunction. Front Cell Neurosci. 2021;15:661838.
83. Mills PJ, Kania-Korwel I, Fagan J, McEvoy LK, Laughlin GA, Barrett-Connor E. Excretion of the Herbicide Glyphosate in older adults between 1993 and 2016. JAMA. 2017;318:1610–1.
84. von Soosten D, Meyer U, Hüther L, Dänicke S, Lahrssen-Wiederholt M, Schafft H, et al. Excretion pathways and ruminal disappearance of glyphosate and its degradation product aminomethylphosphonic acid in dairy cows. J Dairy Sci. 2016;99:5318–24.
85. Cigala RM, De Stefano C, Irto A, Lanzafame P, Papanikolaou G, Crea F. Environmental behaviour of a pesticide metabolite, the AMPA. Sequestration of Ca2+, Mg2+, Cu2+, Zn2 + and Al3+. Chemosphere. 2022;306:135535.
86. Babić Leko M, Mihelčić M, Jurasović J, Nikolac Perković M, Španić E, Sekovanić A, et al. Heavy Metals and Essential Metals Are Associated with Cerebrospinal Fluid biomarkers of Alzheimer's Disease. Int J Mol Sci. 2022;24:467.
87. Doroszkiewicz J, Farhan JA, Mroczko J, Winkel I, Perkowski M, Mroczko B. Common and Trace metals in Alzheimer's and Parkinson's diseases. Int J Mol Sci. 2023;24:15721.

88. DiSabato DJ, Quan N, Godbout JP. Neuroinflammation: the devil is in the details. J Neurochem. 2016;139(Suppl 2):136–53.
89. Maddalon A, Iulini M, Galbiati V, Colosio C, Mandić-Rajčević S, Corsini E. Direct effects of Glyphosate on in Vitro T Helper Cell differentiation and cytokine production. Front Immunol. 2022;13:854837.
90. Kwiatkowska M, Michałowicz J, Jarosiewicz P, Pingot D, Sicińska P, Huras B, et al. Evaluation of apoptotic potential of glyphosate metabolites and impurities in human peripheral blood mononuclear cells (in vitro study). Food Chem Toxicol Int J Publ Br Ind Biol Res Assoc. 2020;135:110888.
91. He Y, Xiong F, Qian Y, Xu K, Pu Y, Huang J, et al. Hematological effects of glyphosate in mice revealed by traditional toxicology and transcriptome sequencing. Environ Toxicol Pharmacol. 2022;92:103866.
92. Pandey A, Dhabade P, Kumarasamy A. Inflammatory effects of Subacute exposure of Roundup in Rat Liver and Adipose tissue. Dose-Response Publ Int Hormesis Soc. 2019;17:1559325819843380.
93. Woźniak E, Reszka E, Jabłońska E, Michałowicz J, Huras B, Bukowska B. Glyphosate and AMPA induce alterations in expression of genes involved in chromatin Architecture in Human Peripheral Blood mononuclear cells (in Vitro). Int J Mol Sci. 2021;22:2966.
94. Bettcher BM, Fitch R, Wynn MJ, Lalli MA, Elofson J, Jastrzab L, et al. MCP-1 and eotaxin-1 selectively and negatively associate with memory in MCI and Alzheimer's disease dementia phenotypes. Alzheimers Dement Amst Neth. 2016;3:91–7.
95. Güzel M, Nazıroğlu M, Akpınar O, Çınar R. Interferon Gamma-mediated oxidative stress induces apoptosis, Neuroinflammation, Zinc Ion Influx, and TRPM2 Channel activation in neuronal cell line: Modulator Role of Curcumin. Inflammation. 2021;44:1878–94.
96. Zhang J, He H, Qiao Y, Zhou T, He H, Yi S, et al. Priming of microglia with IFN-γ impairs adult hippocampal neurogenesis and leads to depression-like behaviors and cognitive defects. Glia. 2020;68:2674–92.
97. Chakrabarty P, Li A, Ceballos-Diaz C, Eddy JA, Funk CC, Moore B, et al. IL-10 alters immunoproteostasis in APP mice, increasing plaque burden and worsening cognitive behavior. Neuron. 2015;85:519–33.
98. Chakrabarty P, Tianbai L, Herring A, Ceballos-Diaz C, Das P, Golde TE. Hippocampal expression of murine IL-4 results in exacerbation of amyloid deposition. Mol Neurodegener. 2012;7:36.
99. Taipa R, das Neves SP, Sousa AL, Fernandes J, Pinto C, Correia AP, et al. Proinflammatory and anti-inflammatory cytokines in the CSF of patients with Alzheimer's disease and their correlation with cognitive decline. Neurobiol Aging. 2019;76:125–32.
100. Brosseron F, Krauthausen M, Kummer M, Heneka MT. Body fluid cytokine levels in mild cognitive impairment and Alzheimer's disease: a comparative overview. Mol Neurobiol. 2014;50:534–44.
101. López-González I, Schlüter A, Aso E, Garcia-Esparcia P, Ansoleaga B, LLorens F, et al. Neuroinflammatory signals in Alzheimer disease and APP/PS1 transgenic mice: correlations with plaques, tangles, and oligomeric species. J Neuropathol Exp Neurol. 2015;74:319–44.
102. Yoshiyama Y, Higuchi M, Zhang B, Huang S-M, Iwata N, Saido TC, et al. Synapse loss and microglial activation precede tangles in a P301S tauopathy mouse model. Neuron. 2007;53:337–51.
103. Ismail R, Parbo P, Madsen LS, Hansen AK, Hansen KV, Schaldemose JL, et al. The relationships between neuroinflammation, beta-amyloid and tau deposition in Alzheimer's disease: a longitudinal PET study. J Neuroinflammation. 2020;17:151.
104. Sastre M, Dewachter I, Landreth GE, Willson TM, Klockgether T, van Leuven F, et al. Nonsteroidal anti-inflammatory drugs and peroxisome proliferator-activated receptor-gamma agonists modulate immunostimulated processing of amyloid precursor protein through regulation of beta-secretase. J Neurosci off J Soc Neurosci. 2003;23:9796–804.
105. Sy M, Kitazawa M, Medeiros R, Whitman L, Cheng D, Lane TE, et al. Inflammation induced by infection potentiates tau pathological features in transgenic mice. Am J Pathol. 2011;178:2811–22.
106. Kwiatkowska M, Reszka E, Woźniak K, Jabłońska E, Michałowicz J, Bukowska B. DNA damage and methylation induced by glyphosate in human peripheral blood mononuclear cells (in vitro study). Food Chem Toxicol Int J Publ Br Ind Biol Res Assoc. 2017;105:93–8.
107. Lin X, Kapoor A, Gu Y, Chow MJ, Peng J, Zhao K, et al. Contributions of DNA damage to Alzheimer's Disease. Int J Mol Sci. 2020;21:1666.
108. Coppedè F, Migliore L. DNA damage and repair in Alzheimer's disease. Curr Alzheimer Res. 2009;6:36–47.
109. Hebda-Bauer EK, Simmons TA, Sugg A, Ural E, Stewart JA, Beals JL, et al. 3xTg-AD mice exhibit an activated central stress axis during early-stage pathology. J Alzheimers Dis JAD. 2013;33:407–22.
110. Baeta-Corral R, Giménez-Llort L. Bizarre behaviors and risk assessment in 3xTg-AD mice at early stages of the disease. Behav Brain Res. 2014;258:97–105.
111. Sterniczuk R, Antle MC, Laferla FM, Dyck RH. Characterization of the 3xTg-AD mouse model of Alzheimer's disease: part 2. Behavioral and cognitive changes. Brain Res. 2010;1348:149–55.
112. Hsiao Y-C, Johnson G, Yang Y, Liu C-W, Feng J, Zhao H, et al. Evaluation of neurological behavior alterations and metabolic changes in mice under chronic glyphosate exposure. Arch Toxicol. 2024;98:277–88.
113. Hwang TJ, Masterman DL, Ortiz F, Fairbanks LA, Cummings JL. Mild cognitive impairment is associated with characteristic neuropsychiatric symptoms. Alzheimer Dis Assoc Disord. 2004;18:17–21.
114. Li JS, Tun SM, Ficek-Tani B, Xu W, Wang S, Horien CL, et al. Medial amygdalar tau is Associated with Mood symptoms in preclinical Alzheimer's Disease. Biol Psychiatry Cogn Neurosci Neuroimaging. 2024;S2451–9022(24):00200–3.
115. Zhao Q-F, Tan L, Wang H-F, Jiang T, Tan M-S, Tan L, et al. The prevalence of neuropsychiatric symptoms in Alzheimer's disease: systematic review and meta-analysis. J Affect Disord. 2016;190:264–71.
116. España J, Giménez-Llort L, Valero J, Miñano A, Rábano A, Rodriguez-Alvarez J, et al. Intraneuronal beta-amyloid accumulation in the amygdala enhances fear and anxiety in Alzheimer's disease transgenic mice. Biol Psychiatry. 2010;67:513–21.
117. Reyna NC, Clark BJ, Hamilton DA, Pentkowski NS. Anxiety and Alzheimer's disease pathogenesis: focus on 5-HT and CRF systems in 3xTg-AD and TgF344-AD animal models. Front Aging Neurosci. 2023;15:1251075.
118. Zheng Z-H, Tu J-L, Li X-H, Hua Q, Liu W-Z, Liu Y, et al. Neuroinflammation induces anxiety- and depressive-like behavior by modulating neuronal plasticity in the basolateral amygdala. Brain Behav Immun. 2021;91:505–18.
119. Inagaki TK, Muscatell KA, Irwin MR, Cole SW, Eisenberger NI. Inflammation selectively enhances amygdala activity to socially threatening images. NeuroImage. 2012;59:3222–6.
120. Gehring TV, Luksys G, Sandi C, Vasilaki E. Detailed classification of swimming paths in the Morris Water Maze: multiple strategies within one trial. Sci Rep. 2015;5:14562.

Publisher's note